

# Supporting Information

## Advancing non-isocyanate polyurethane foams: *exo*-vinylene cyclic carbonate–amine chemistry enabling room-temperature reactivity and fast self-blowing

Maksim Makarov,<sup>1</sup> Maxime Bourguignon,<sup>1</sup> Bruno Grignard,<sup>\*,1,2</sup> and Christophe Detrembleur<sup>\*,1,3</sup>

<sup>1</sup>Center for Education and Research on Macromolecules (CERM), CESAM Research Unit, University of Liege, Sart-Tilman B6a, 4000 Liege, Belgium

<sup>2</sup>FRITCO<sub>2</sub>T Platform, University of Liege, Sart-Tilman B6a, 4000 Liege, Belgium

<sup>3</sup>WEL Research Institute, avenue Pasteur, 6, 1300 Wavre, Belgium

### Table of Contents

<b>1. Abbreviations</b>	<b>3.4.3. Foam extraction analysis</b>
<b>2. Foaming Formulations</b>	<b>3.5. Versatility of the technology</b>
<b>3. Results and Discussions</b>	<b>3.5.1. Formulations with different <math>\alpha</math>CCs</b>
<b>3.1. <math>\alpha</math>CC aminolysis exotherm and its impact on foaming</b>	<b>3.5.1.1. FT-IR analysis</b>
<b>3.1.1. Model reaction <math>\alpha</math>CC aminolysis exotherm</b>	<b>3.5.1.2. DSC analysis</b>
<b>3.2 Characterization of NIPUFs prepared with different contents of <math>\alpha</math>CC</b>	<b>3.5.1.3. TGA analysis</b>
<b>3.2.1.DSC analysis</b>	<b>3.5.2. Formulations with different amines mixture</b>
<b>3.2.2.TGA analysis</b>	<b>3.5.2.1. FT-IR analysis</b>
<b>3.2.3. FT-IR analysis</b>	<b>3.5.2.2. DSC analysis</b>
<b>3.3. Characterization of NIPUFs prepared with different contents of water</b>	<b>3.5.2.3. TGA analysis</b>
<b>3.3.1. DSC analysis</b>	<b>3.5.4.4. Exotherm recorded depending on amine ratio of TREN to diamine used in the formulation</b>
<b>3.3.2. TGA analysis</b>	<b>3.6. Compression tests</b>
<b>3.3.3. FT-IR analysis</b>	<b>4. <math>\alpha</math>CC monomer synthesis</b>
<b>3.4. Foaming mechanism</b>	<b>4.1. DMACC monomer synthesis</b>
<b>3.4.1. Foaming Equivalents Kinetics</b>	<b>4.2. CHACC monomer synthesis</b>
<b>3.4.2. Equimolar (Competitive) Kinetics</b>	<b>4.3. iBuMACC monomer synthesis</b>
	<b>4.4. MPACC monomer synthesis</b>

# Supporting Information

## 1. Abbreviations

**Table S1.** Abbreviations.

General			
Abbreviation	Name	Abbreviation	Name
Cat	Catalyst	NIPUF	Non-isocyanate polyurethane foam
CC	Cyclic carbonate	T <sub>g</sub>	Glass transition temperature
5CC	Five-membered cyclic carbonate group	T <sub>d 5%</sub>	Degradation temperature (5% by weight loss)
min	Minute	T <sub>onset</sub>	Estimated start of degradation
h	Hour	GC	Gel content
sec	Second	Eq	Equivalent
αCC	Exo-vinylene cyclic carbonate	FG	Functional Group
Characterization techniques			
FT-IR	Fourier transform infrared spectroscopy	TGA	Thermogravimetric analysis
NMR	Nuclear magnetic resonance	SEM	Scanning electron microscopy
DSC	Differential scanning calorimetry		
Chemicals and polymers			
NIPU	Non-Isocyanate Polyurethane	DMACC	4,4-Dimethyl-5-methylene-1,3-dioxolan-2-one
PU	Polyurethane	<i>i</i> -BuMACC	4-isobutyl-4-methyl-5-methylene-1,3-dioxolan-2-one
PrC	Propylene carbonate	CHACC	4-methylene-1,3-dioxaspiro[4.5]decan-2-one
TREN	Tris(2-aminoethyl)amine	EDR-148	2,2'-(ethane-1,2-diylbis(oxy))bis(ethan-1-amine)
TMPTC	Trimethylol propane triglycidyl carbonate	IPDA	Isophorone diamine
mXDA	m-Xylylenediamine	HMDA	Hexamethylenediamine
HDPE	High density polyethylene	MPACC	4-methyl-5-methylene-4-phenyl-1,3-dioxolan-2-one

## Supporting Information

### 2. Foaming Formulations

Formulation equivalents were computed using the equation:  $(n(5CC) - n(H_2O)) + n(\alpha CC) = n(NH_2)$ , where  $n(5CC)$  represents total mol of 5-membered cyclic carbonate groups,  $n(H_2O)$  represents mol of water,  $n(\alpha CC)$  represents the number of moles of  $\alpha CC$ , and  $n(NH_2)$  represents total amine group mol. A hydrotalcite filler (10 wt% compared to the cyclic carbonate monomer, TMPTC). This amount was identified as optimal in [36]) was incorporated, while the catalyst was proportioned at 50 mol% of water.

**Table S2.** NIPUF formulations expressed in mmol.

Formulation	Formulation components in mmol						
	TMPTC (5CC)	Amine 1 (NH <sub>2</sub> )	Amine 2 (NH <sub>2</sub> )	$\alpha CC$	H <sub>2</sub> O	Cat.	Filler**
F1	TMPTC 207.19	TREN 196.83	-	DMACC 0.72 *	31.08	KOH 15.54	HTC
F2	TMPTC 207.19	TREN 207.19	-	DMACC 31.08	31.08	KOH 15.54	HTC
F3	TMPTC 207.19	TREN 217.55	-	DMACC 1.44 *	31.08	KOH 15.54	HTC
F4	TMPTC 207.19	TREN 227.91	-	DMACC 51.80	31.08	KOH 15.54	HTC
F5	TMPTC 207.19	TREN 238.27	-	DMACC 62.16 *	31.08	KOH 15.54	HTC
F6	TMPTC 207.19	TREN 238.27	-	DMACC 51.80	20.72	KOH 10.36	HTC
F7	TMPTC 207.19	TREN 217.55	-	DMACC 51.80	41.44	KOH 20.72	HTC
F8	TMPTC 207.19	TREN 166.79	mXDA 71.48	DMACC 51.80	20.72	KOH 10.36	HTC
F9	TMPTC 207.19	TREN 166.79	HMDA 71.48	DMACC 51.80	20.72	KOH 10.36	HTC
F10	TMPTC 207.19	TREN 166.79	EDR-148 71.48	DMACC 51.80	20.72	KOH 10.36	HTC
F11	TMPTC 207.19	TREN 166.79	IPDA 71.48	DMACC 51.80	20.72	KOH 10.36	HTC
F12	TMPTC 207.19	TREN 238.27	-	<i>i</i> -BuMACC 51.80	20.72	KOH 10.36	HTC
F13	TMPTC 207.19	TREN 238.27	-	CHACC 51.80	20.72	KOH 10.36	HTC
F14	TMPTC 207.19	TREN 238.27	-	MPACC 51.80	20.72	KOH 10.36	HTC

\* In **2.1**. Same formulation applied with  $\alpha CC$  substituted with TMPTE.

\*\* The filler was used with a 10 wt% to poly(cyclic carbonate).

## Supporting Information

**Table S3.** NIPUF formulations expressed in compound mass (g).

Formulation	Masses of formulation components (g)						
	TMPTC (5CC)	Amine 1 (NH <sub>2</sub> )	Amine 2 (NH <sub>2</sub> )	$\alpha$ CC	H <sub>2</sub> O	Cat.	Filler**
F1	TMPTC 30	TREN 9.59	-	DMACC 2.65 *	0.56	KOH 0.87	HTC 3
F2	TMPTC 30	TREN 10.10	-	DMACC 3.98	0.56	KOH 0.87	HTC 3
F3	TMPTC 30	TREN 10.60	-	DMACC 5.31*	0.56	KOH 0.87	HTC 3
F4	TMPTC 30	TREN 11.11	-	DMACC 6.64	0.56	KOH 0.87	HTC 3
F5	TMPTC 30	TREN 11.61	-	DMACC 7.96 *	0.56	KOH 0.87	HTC 3
F6	TMPTC 30	TREN 11.61	-	DMACC 6.64	0.37	KOH 0.58	HTC 3
F7	TMPTC 30	TREN 10.60	-	DMACC 6.64	0.75	KOH 1.16	HTC 3
F8	TMPTC 30	TREN 8.13	mXDA 4.87	DMACC 6.64	0.37	KOH 0.58	HTC 3
F9	TMPTC 30	TREN 8.13	HMDA 4.15	DMACC 6.64	0.37	KOH 0.58	HTC 3
F10	TMPTC 30	TREN 8.13	EDR-148 5.30	DMACC 6.64	0.37	KOH 0.58	HTC 3
F11	TMPTC 30	TREN 8.13	IPDA 6.08	DMACC 6.64	0.37	KOH 0.58	HTC 3
F12	TMPTC 30	TREN 9.68	-	<i>i</i> -BuMACC 8.82	0.37	KOH 0.58	HTC 3
F13	TMPTC 30	TREN 11.61	-	CHACC 8.71	0.37	KOH 0.58	HTC 3
F14	TMPTC 30	TREN 11.61	-	MPACC 9.85	0.37	KOH 0.58	HTC 3

\* In **2.1**. Same formulation applied with  $\alpha$ CC substituted with TMPTE.

\*\* The filler was used with a 10 wt% to poly(cyclic carbonate).

### 3.Results and Discussions

#### 3.1. $\alpha$ CC aminolysis exotherm and its impact on foaming

##### 3.1.1. Model reaction $\alpha$ CC aminolysis exotherm

An aluminum heating block with sample slots equipped with a thermal probe was placed on a magnetic stirrer hotplate. A 40 mL sample vial, equipped with a separate Martindale TT6K thermal probe, was placed in the aluminum heating block. Then, DMACC (3 g, 23 mmol, 1 eq.) was added to the sample vial along with a magnetic stirrer bar. The sample vial was heated to 30 °C to melt the DMACC, and simultaneously, 1-heptylamine (2.7 g, 23 mmol, 1 eq.) was added to the sample vial. The exotherm was recorded (**Figure S1**).

## Supporting Information

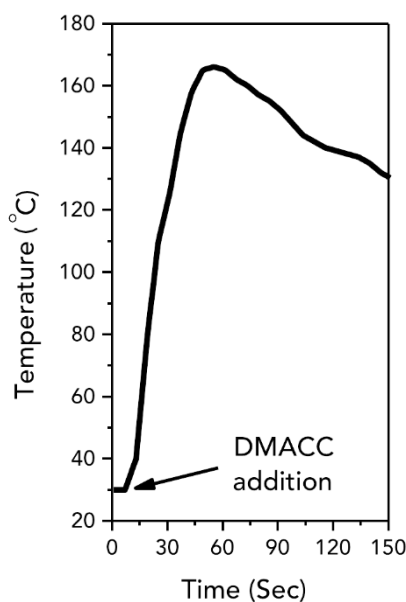


**Figure S1.** Temperature vs. time plot in pure DMACC aminolysis reaction. The arrow points to the moment of temperature increase that reflects the addition of 1-heptylamine.

### 3.2. Characterization of NIPUFs prepared with different contents of $\alpha$ CC

**Table S4.** Characterization of NIPUFs made with formulations **F2-5**, utilizing different DMACC ( $\alpha$ CC) contents in the formulation. (See Table 1, and S2-3 in ESI for all formulations; section 6.3.3. for NIPUF synthesis conditions).

Entry	DMACC eq. to 5CC	Total density, ( $\text{kg} \times \text{m}^{-3}$ )	Inner average density, ( $\text{kg} \times \text{m}^{-3}$ )	Gel content, %	$T_{g, \text{eq.}}$	$T_{g, \text{dry}}$	$T_{d, 5\%}$
F2	0.15	323	$152 \pm 12$	97	36	47.5	250
F3	0.2	230	$102 \pm 14$	93	31.5	47	248
F4	0.25	188	$78 \pm 15$	91	31	46.5	248
F5	0.3	173	$58 \pm 15$	89	28	46	248

## Supporting Information

### 3.2.1.DSC analysis

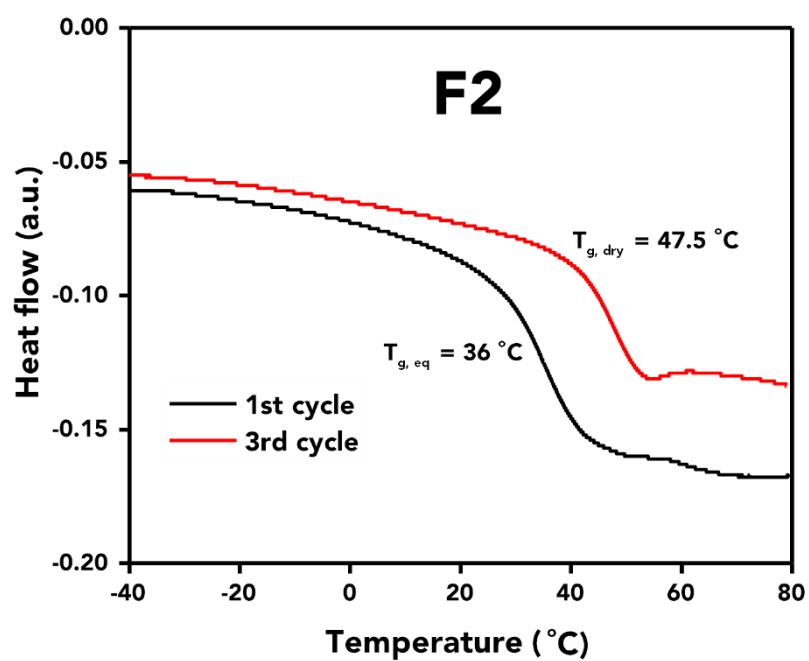


**Figure S2.** DSC thermogram of formulation **F2**. (0.15 aCC eq. to 5CC).

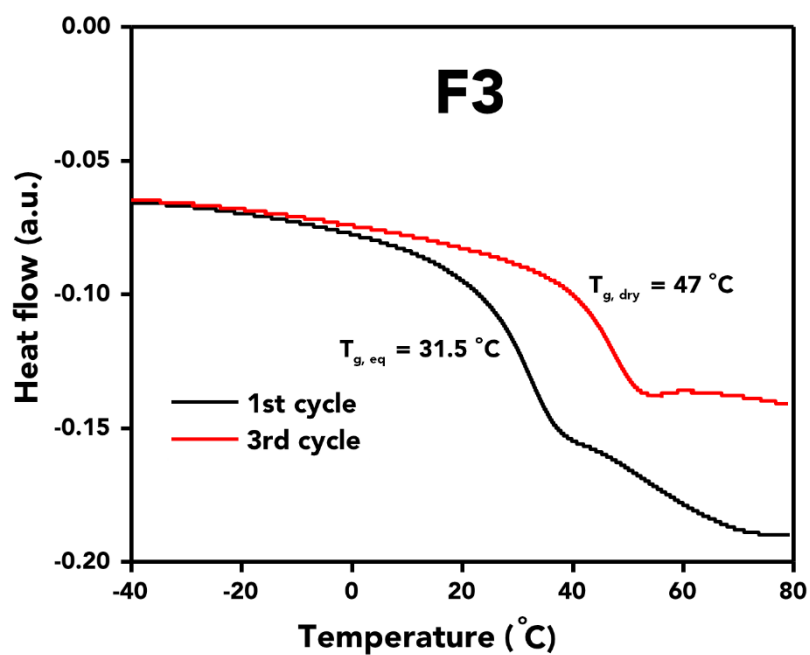


**Figure S3.** DSC thermogram of formulation **F3**. (0.20 aCC eq. to 5CC).

## Supporting Information

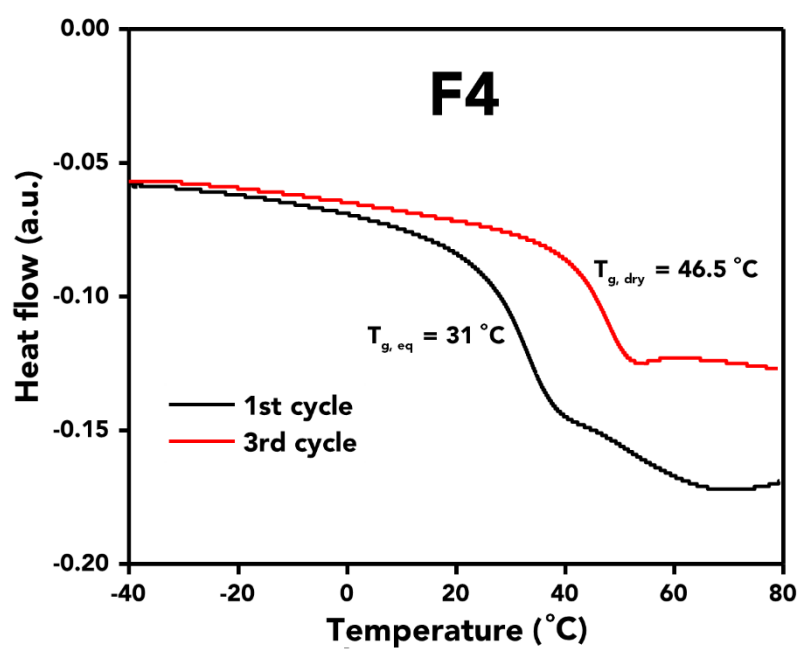


**Figure S4.** DSC thermogram of formulation **F4**. (0.25 aCC eq. to 5CC).

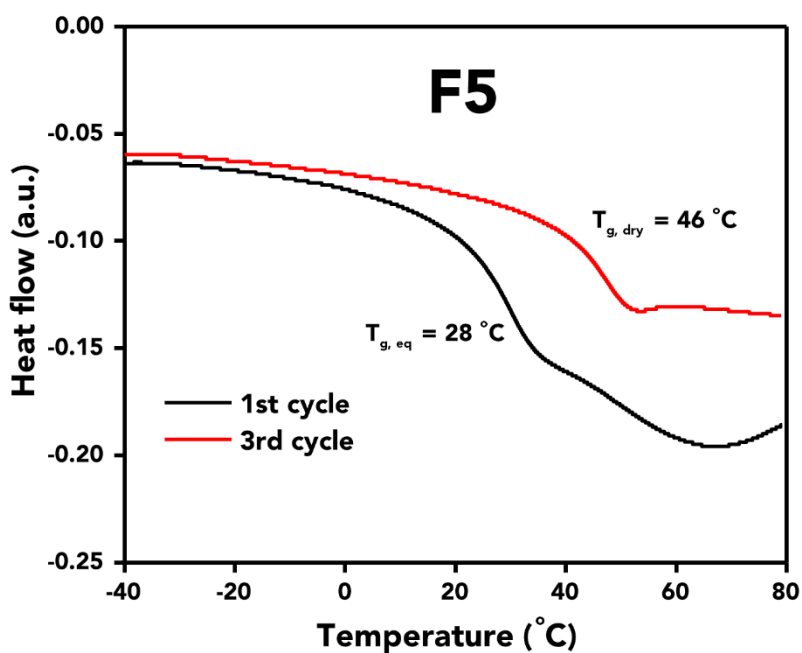


**Figure S5.** DSC thermogram of formulation **F5**. (0.30 aCC eq. to 5CC).

## Supporting Information

### 3.2.2.TGA analysis

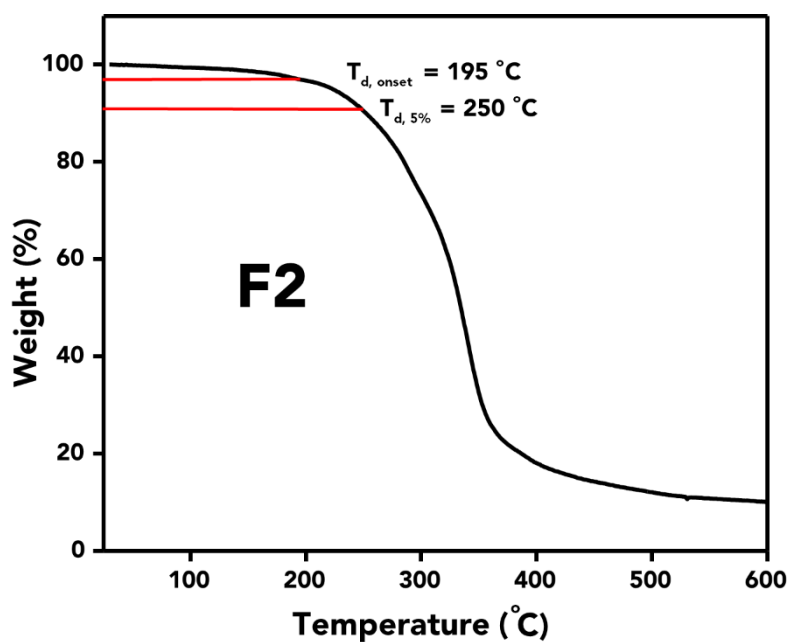


**Figure S6.** TGA thermogram of formulation **F2**. (0.15 aCC eq. to 5CC).

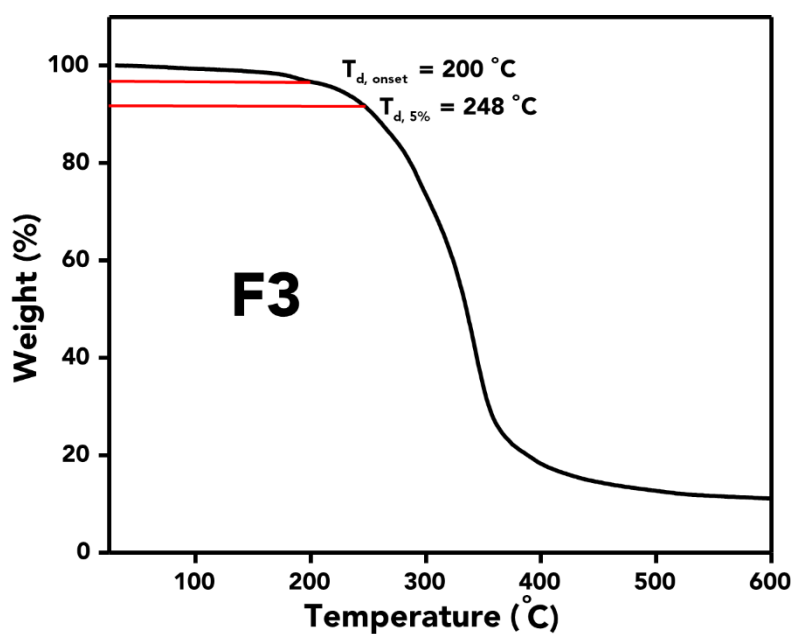


**Figure S7.** TGA thermogram of formulation **F3**. (0.20 aCC eq. to 5CC).



## Supporting Information

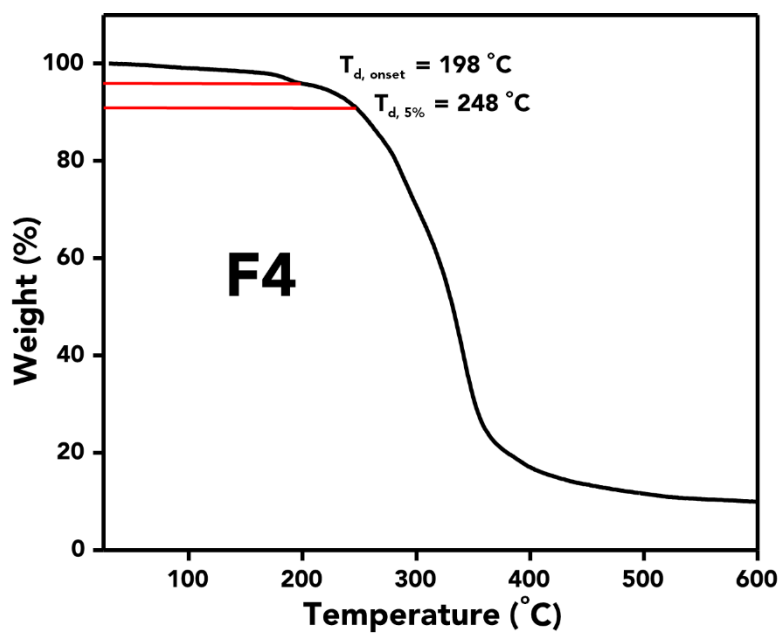


**Figure S8.** TGA thermogram of formulation **F4**. (0.25 aCC eq. to 5CC).

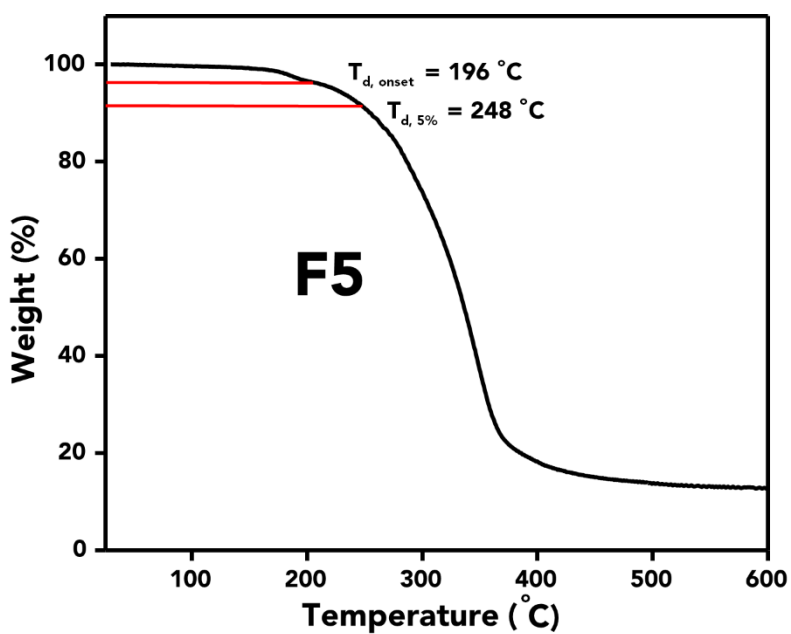


**Figure S9.** TGA thermogram of formulation **F5**. (0.30 aCC eq. to 5CC).

## Supporting Information

### 3.2.3. FT-IR analysis

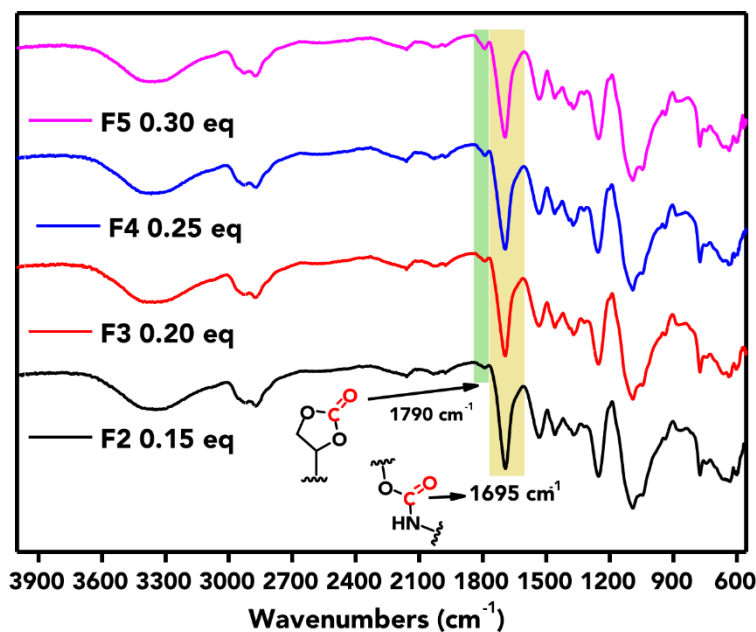


**Figure S10.** Stacked FT-IR spectra of formulations **F2-F5**, where DMACC (aCC) equivalents varied from 0.15 to 0.30 eq. to 5CC respectively.

### 3.3. Characterization of NIPUFs prepared with different contents of water

**Table S5.** Characterization of NIPUFs made with formulations **F4**, **F6-7**, utilizing different water contents in the formulation; \*Since 0.15 water eq. per 5CC groups were used in formulation **F4**, its data was used as a reference.

Entry	Water eq. to 5CC	Total density, (kg × m <sup>-3</sup> )	Inner average density, (kg × m <sup>-3</sup> )	Gel content, %	T <sub>g</sub> , eq.	T <sub>g</sub> , dry	T <sub>d</sub> , 5%
F4*	0.15	188	78 ± 15	91	31	46	248
F6	0.10	233	128 ± 15	98	31.5	46.5	244
F7	0.2	168	65 ± 15	89	26	45	230

## Supporting Information

### 3.3.1. DSC analysis

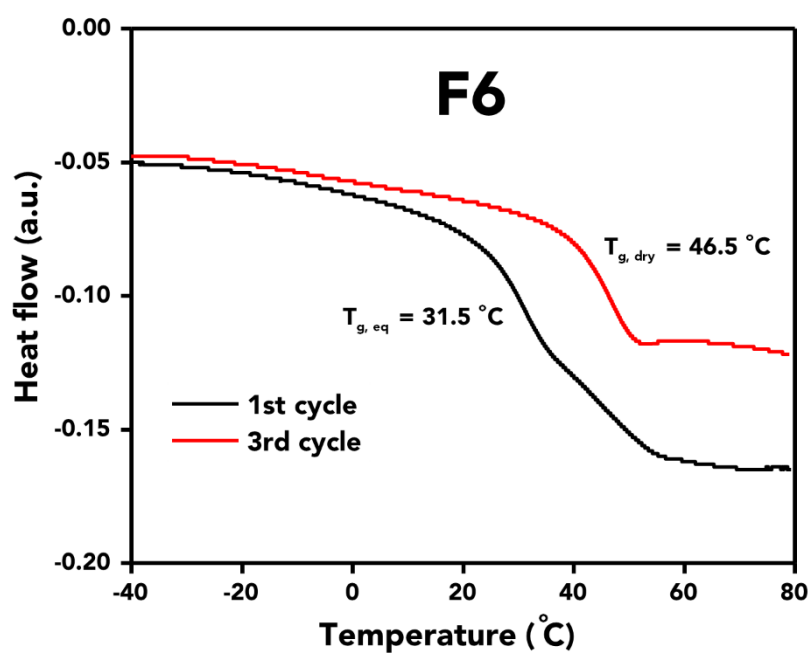


**Figure S11.** DSC thermogram of formulation **F6**. (0.10 water eq. to 5CC).

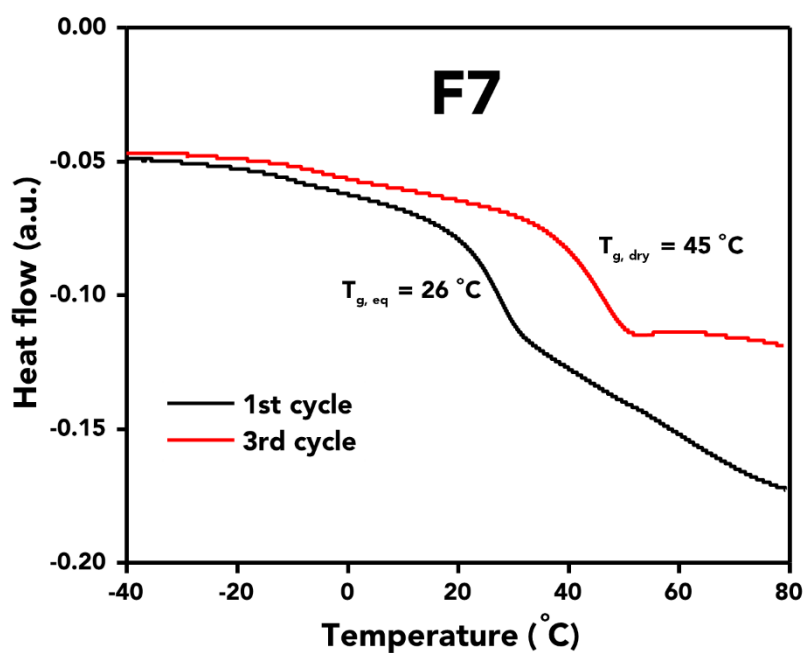


**Figure S12.** DSC thermogram of formulation **F7**. (0.20 water eq. to 5CC).

## Supporting Information

### 3.3.2. TGA analysis

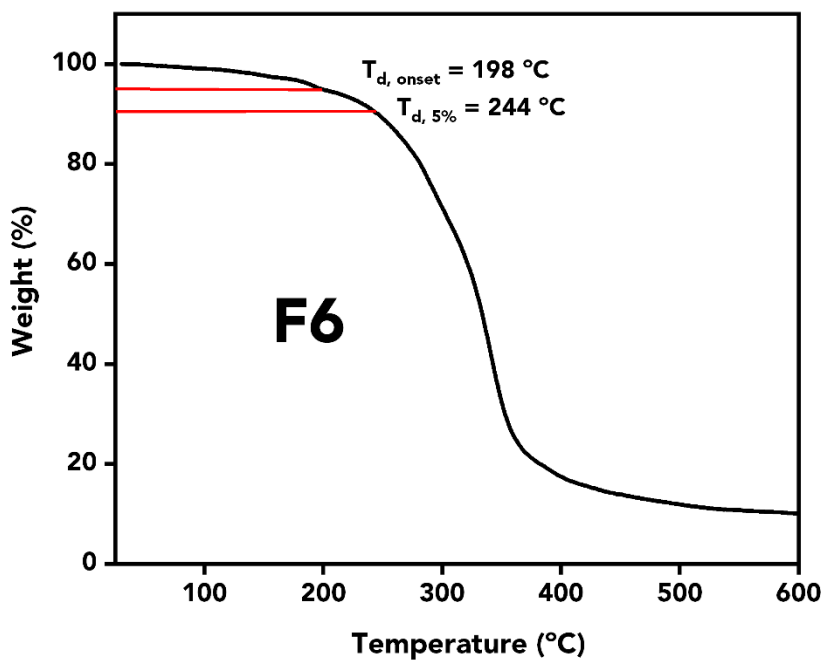


**Figure S13.** TGA thermogram of formulation **F6**. (0.10 water eq. to 5CC).

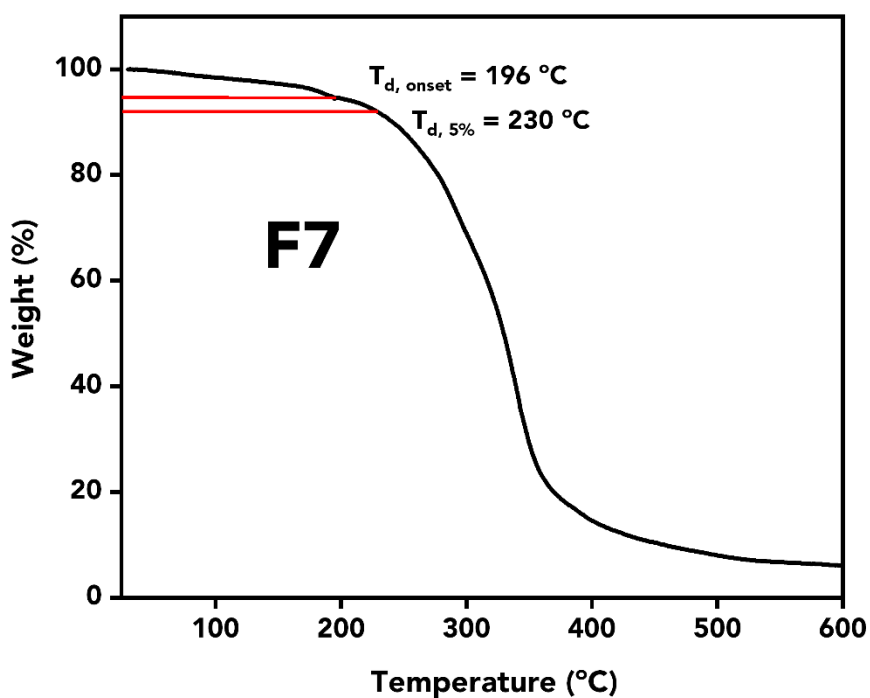


**Figure S14.** TGA thermogram of formulation **F7**. (0.20 water eq. to 5CC).

## Supporting Information

### 3.3.3. FT-IR analysis

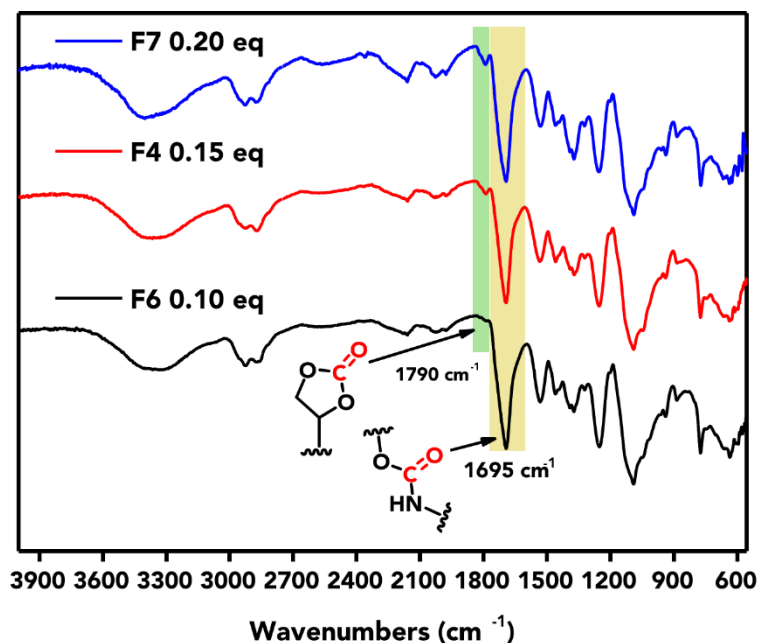


**Figure S15.** Stacked FT-IR spectra of formulations **F4**, **F6** and **F7**, where 0.15, 0.10 and 0.20 water equivalents to 5CC were applied, respectively.

### 3.4. Foaming mechanism.

#### 3.4.1. Foaming Equivalents Kinetics

On a magnetic stirrer hotplate, the aluminum heating block was equipped with a thermal probe. In a 40 mL sample vial, equipped with the Matindale TT6K thermal probe, was put in the aluminum heating block. In the sample vial, equipped with a magnetic stirrer bar, DMACC (1 g, 8 mmol, 0.25 eq.) was dissolved in PrC (3.19 g, 31 mmol, 1 eq.). Then, simultaneously, 1-heptylamine (4.14 g, 36 mmol, 1.15 eq.) with KOH (0.087 g, 1.55 mmol, 0.05 eq.) dissolved in H<sub>2</sub>O (0.056 g, 3.1 mmol, 0.1 eq.) was added to the sample vial. The rapid exotherm was recorded (**follow the orange line in Figure 7B**). With respect to the sampling time of 0.5 min, 1 min, 2 min, 5 min, 10 min, and 15 min, 0.13 mL of the solution was collected and quenched with 0.05 mL of 99.5% acetic acid. The quenched samples were analyzed via <sup>1</sup>H-NMR.

## Supporting Information

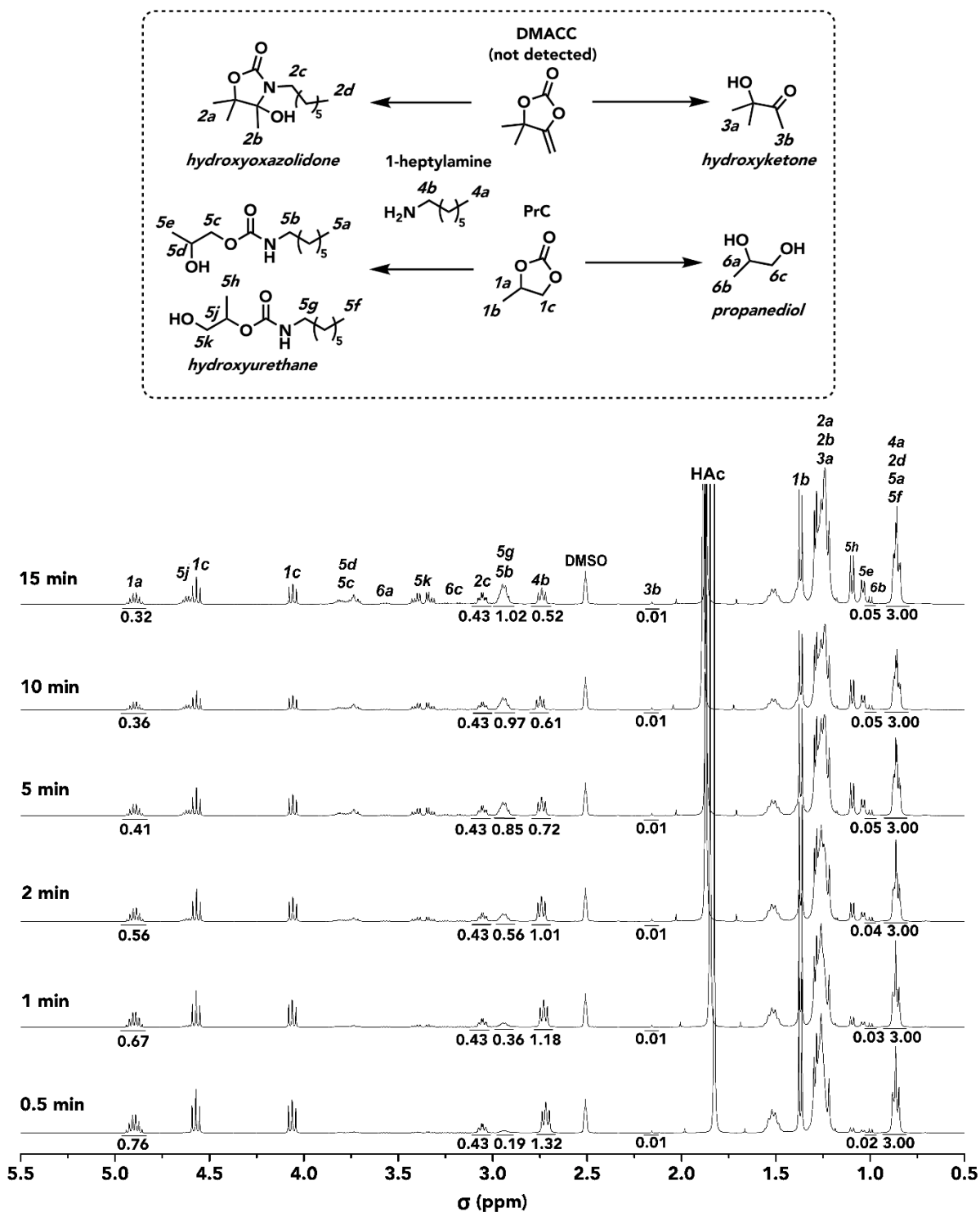


**Figure S16.** Stacked  $^1\text{H}$ -NMR spectra of quenched reaction mixture samples, collected at a set time, from the model reaction carried out in foaming reaction equivalents. Note that DMACC peaks are not present, as it was fully consumed before the first sample was collected.

## Supporting Information

The yield of products and consumption of reactants was calculated by a reference multiplet at 0.85 ppm, representing the methyl group of 1-heptylamine. Therefore, a molar ratio of 1.15 : 1.00 (1-heptylamine : PrC) must be kept in mind during product formation and reactant consumption yield calculation (i.e., if the methyl peak is considered as 3.00, meaning 3H, 100% of 1H on other molecules is 0.87).

Yields of oxazolidone and hydroxyketone were calculated accordingly to the following formulas:

$$\text{Yield}_{(\text{oxazolidone})} = \frac{\frac{i^{2c}}{2}}{\frac{i^{\text{Reference}}}{3}} \times 100\%; \quad \text{Yield}_{(\text{hydroxyketone})} = \frac{\frac{i^{3b}}{3}}{i^{\text{Reference}}} \times 100\%;$$

$$\text{Yield}_{(\text{hydroxyurethane})} = \frac{\frac{i^{5g+5b}}{2}}{\frac{i^{\text{Reference}}}{3}} \times 100\%; \quad \text{Yield}_{(\text{propanediol})} = \frac{\frac{i^{6a}}{1}}{\frac{i^{\text{Reference}}}{3}} 100\%;$$

Where  $i^{\text{Reference}} = 4a+2d+5a+5f$  multiplet signal integration.

### 3.4.2. Equimolar (Competitive) Kinetics

In an equimolar (competitive) assay (*see Figure S17*), the nucleophiles (amine and water) were maintained at equimolar ratios with each other and with the αCC to see how yields of aminolysis and hydrolysis products will distribute in such a system. After the simultaneous addition of nucleophiles, a rapid heat release was recorded, reaching a maximum of 130°C, followed by gradual cooling of the reaction mixture (*see Figure S18*). <sup>1</sup>H-NMR analysis of the reaction mixture sample collected after 30 seconds of reaction showed that DMACC was fully converted, resulting in the aminolysis product hydroxyoxazolidone (80% yield) and the hydrolysis product hydroxyketone (20% yield) (*see Figure S19*). No oxo-urethane intermediate was detected, suggesting its immediate conversion to oxazolidone due to the elevated reaction temperature caused by the exothermic reaction<sup>[41,42]</sup>. The important information derived from this assignment is that, although αCC hydrolysis does occur in this system, its yield is significantly lower compared to the formation of hydroxyoxazolidone. This indicates that aminolysis is the predominant reaction under the conditions studied.

**Procedure:** An aluminum heating block with a thermal probe was placed on a magnetic stirrer hotplate. A 40 mL sample vial, equipped with a separate Martindale TT6K thermal probe, was placed in the aluminum heating block. DMACC (3 g, 23 mmol, 1 eq.) and a magnetic stirrer bar were then added to the sample vial. The sample vial was heated to 30 °C to melt the DMACC, and simultaneously, 1-heptylamine (2.7 g, 23 mmol, 1 eq.) and KOH (0.65 g, 11.5 mmol, 0.5 eq.) dissolved in H<sub>2</sub>O (0.42 mL, 23 mmol, 1 eq.) were added to the sample vial. The rapid exotherm was recorded (*Figure S17*). Samples of 0.13 mL were collected at 0.25 min, 0.5 min, 1 min, 5 min, 10 min, and 15 min and quenched with 0.05 mL of 99.5% acetic acid. The quenched samples were analyzed via NMR (*Figure S18*).

## Supporting Information

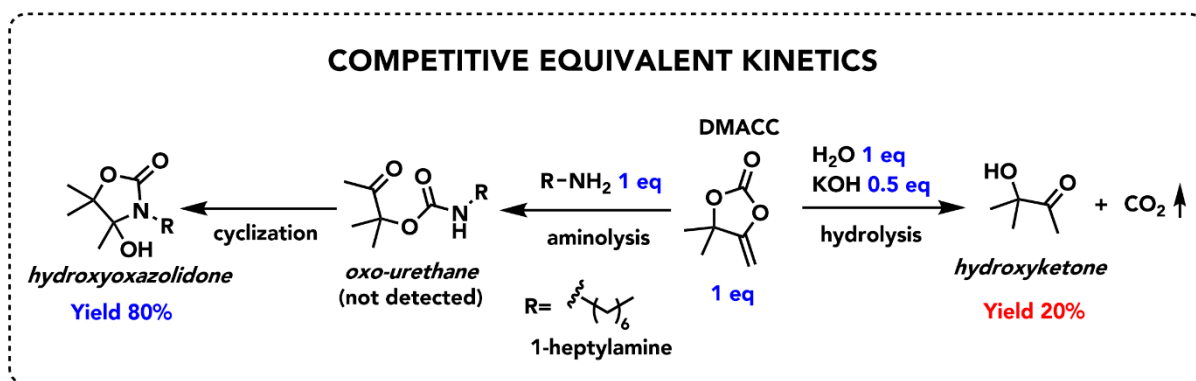


**Figure S17.** Kinetic studies of DMACC aminolysis vs. DMACC hydrolysis. Scheme of in situ reactions carried out in equimolar (competitive) conditions.

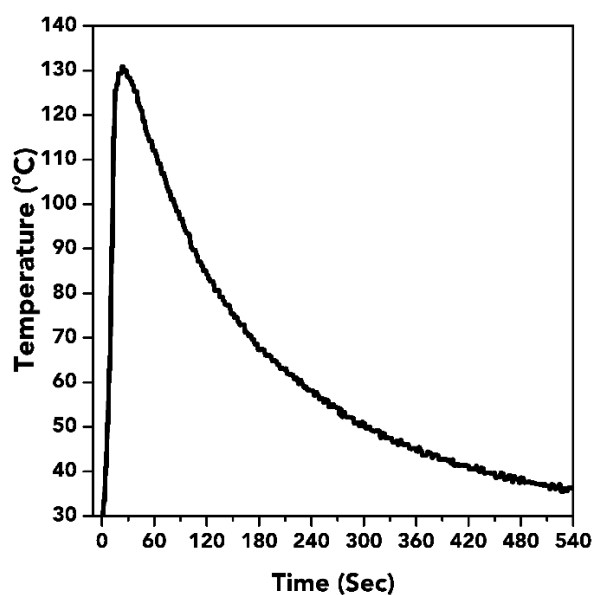


**Figure S18.** Temperature vs. time plot in competitive equivalents model reaction.



## Supporting Information

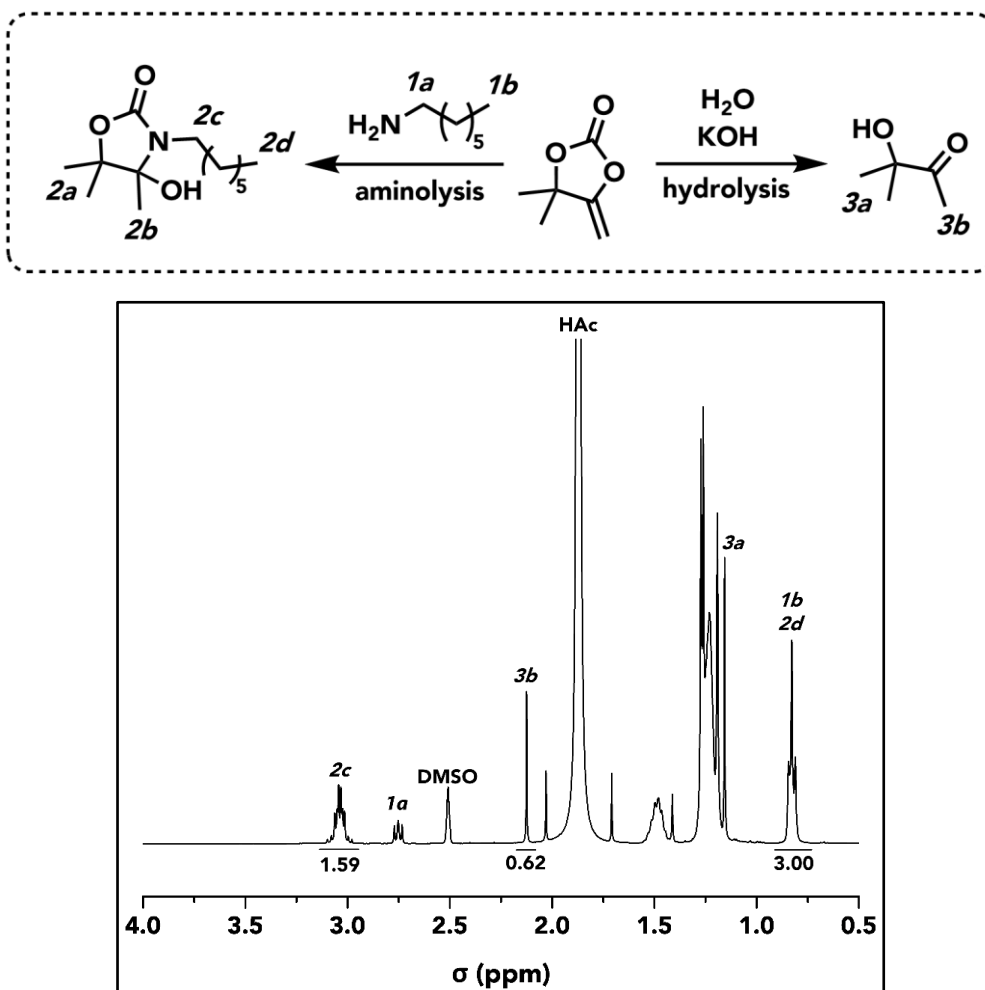


**Figure S19.** Assigned  $^1\text{H}$ -NMR spectra of a quenched sample of a reaction mixture of DMACC aminolysis and DMACC hydrolysis reactions in competitive equivalents, collected 30 sec after the addition of nucleophiles. Aminolysis product (hydroxyoxazolidone) yield = 80%; hydrolysis product (hydroxyketone) yield = 20%.

Yields of oxazolidone and hydroxyketone were calculated accordingly to the following formulas:

$$\text{Yield}_{(\text{oxazolidone})} = \frac{\frac{i^{2c}}{2}}{\frac{i^{\text{Reference}}}{3}} \times 100\%; \quad \text{Yield}_{(\text{hydroxyketone})} = \frac{i^{3b}}{i^{\text{Reference}}} \times 100\%;$$

Where  $i^{\text{Reference}} = 1b+2d$  integration.

## Supporting Information

### 3.4.3. Foam extraction analysis.

The **F6** formulation foam was fully immersed in a 250 mL glass vial, filled with THF, and placed on the VWR Micro Plate Shaker set on 200 RPM. After 72 h, the extracted solution was isolated and dried under vacuum at 25 °C. The remaining oily residue was analyzed via  $^1\text{H}$  and  $^{13}\text{C}$  NMR.

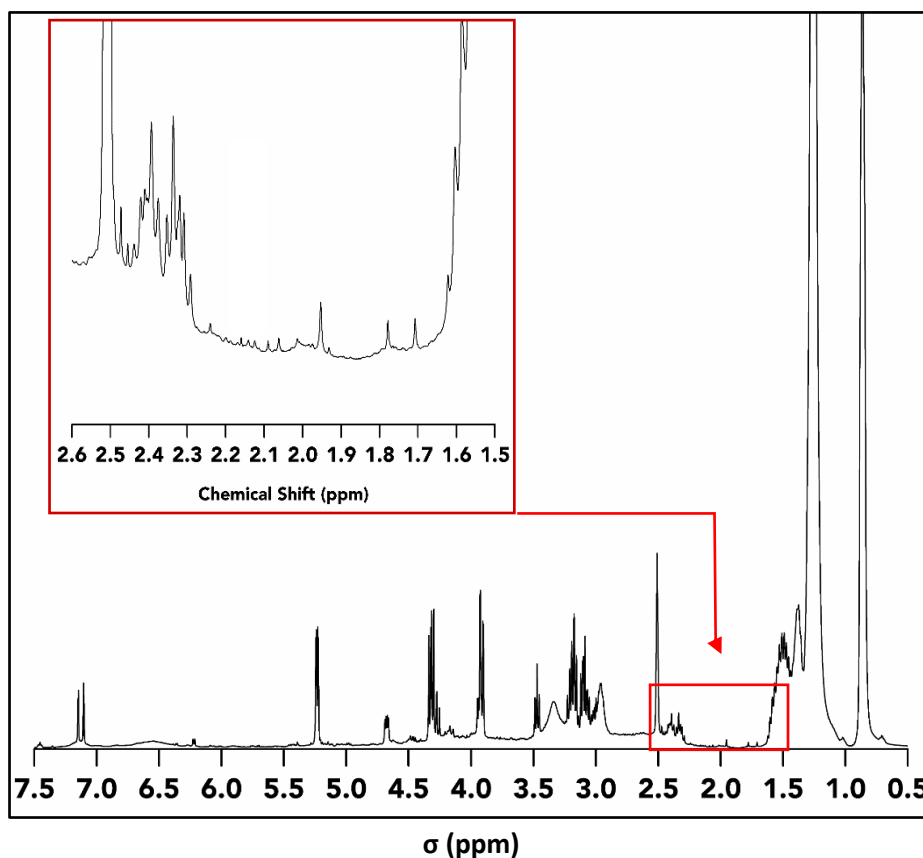


**Figure S20.**  $^1\text{H}$ -NMR spectra of an **F6** formulation foam extract with a zoomed region where the hydroxyketone peak is expected to appear.

## Supporting Information

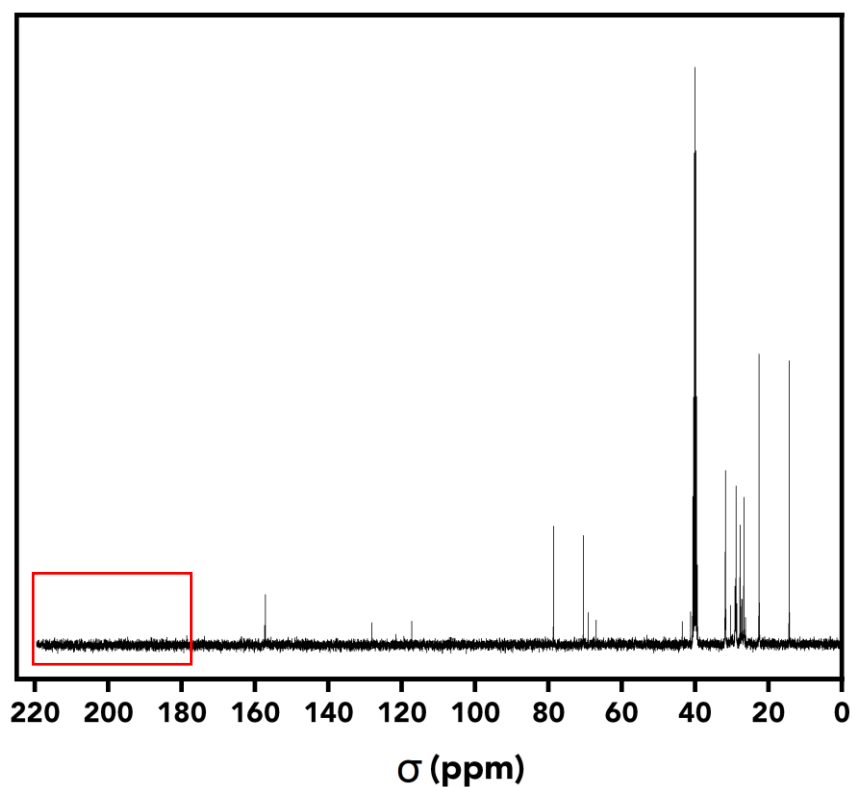


**Figure S21.**  $^{13}\text{C}$ -NMR spectra of an **F6** formulation foam extract with a zoomed region where the hydroxyketone peak is expected to appear.

Accordingly, to the analysis, no hydroxyketone signals were seen on NMR, meaning that even if the side product is formed, its yield is insignificant, thus it can be neglected.

## Supporting Information

### 3.5. Versatility of the technology

#### 3.5.1. Formulations with different $\alpha$ CCs

##### 3.5.1.1. FT-IR analysis

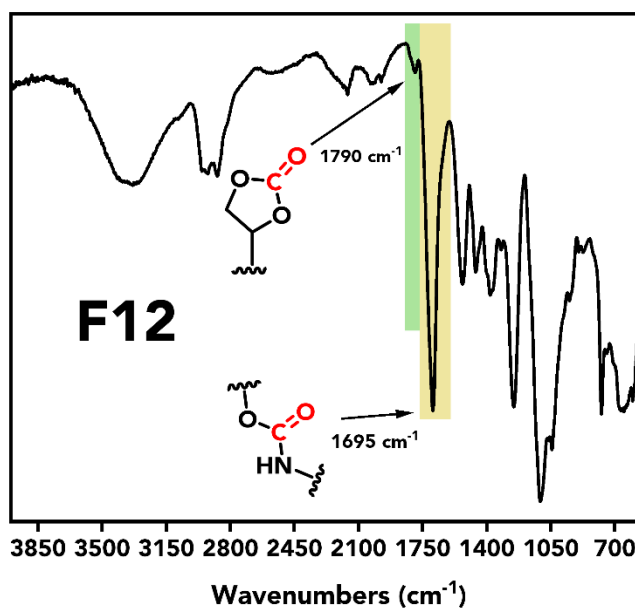


**Figure S22.** FT-IR spectra of formulation **F12**. In this formulation, *i*BuMACC was employed instead of DMACC.

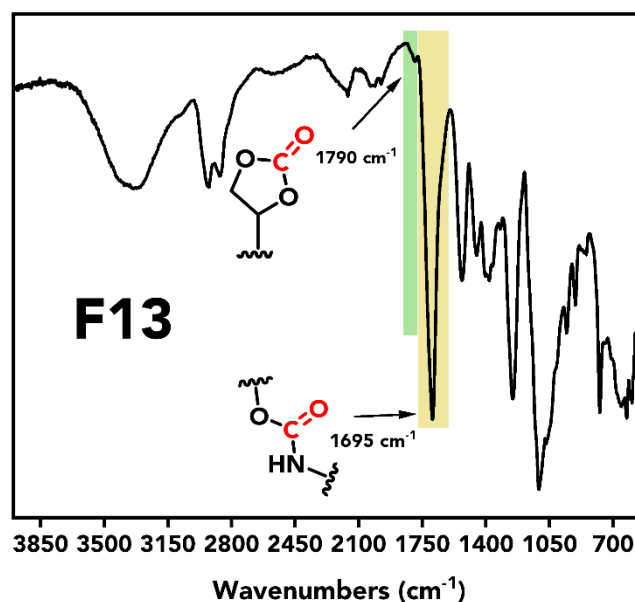


**Figure S23.** FT-IR spectra of formulation **F13**. In this formulation, CHACC was employed instead of DMACC.

## Supporting Information

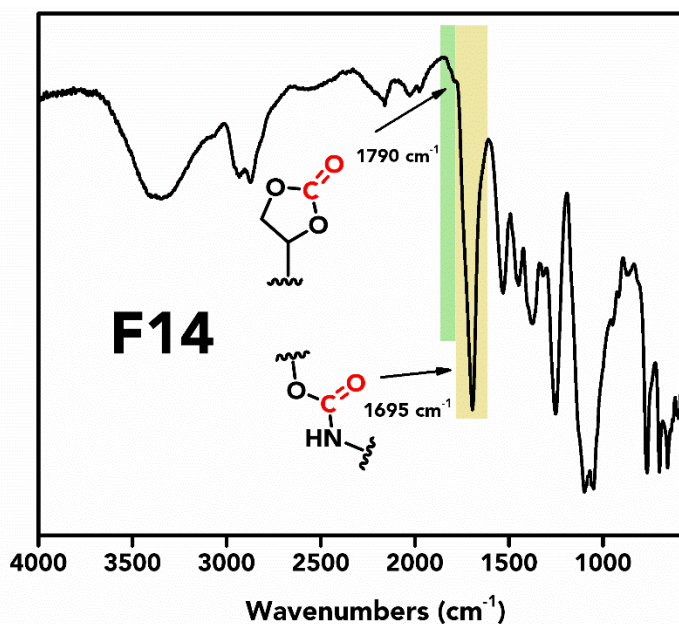


**Figure S24.** FT-IR spectra of formulation **F14**. In this formulation, MPACC was employed instead of DMACC.

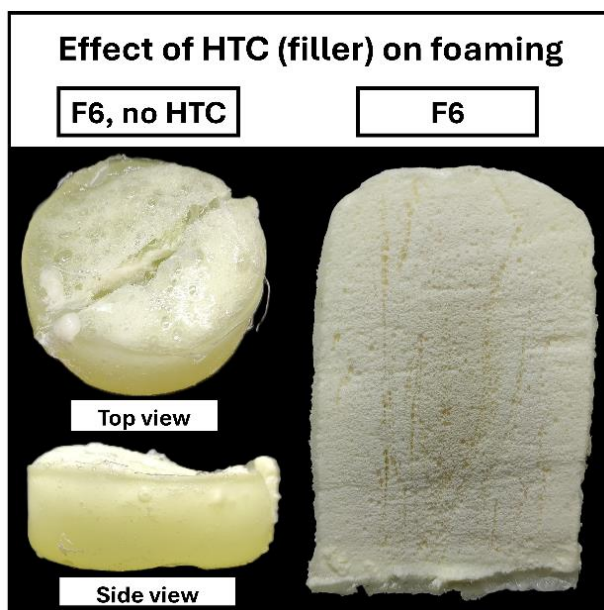


**Figure S25.** Effect of the HTC (filler) on the same NIPUF formulation. Left - **F6** formulation without HTC; Right - **F6** formulation with HTC.

## Supporting Information

### 3.5.1.2. DSC analysis

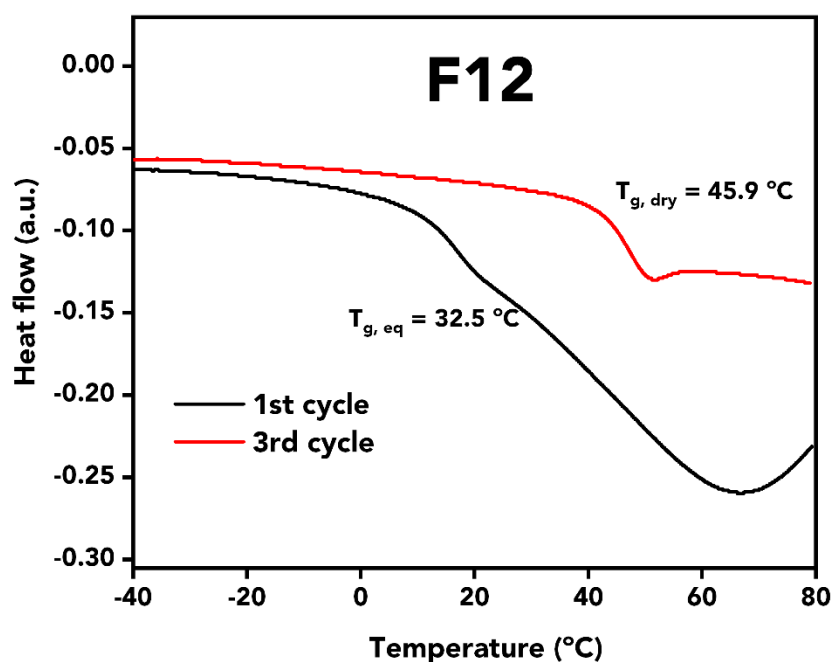


**Figure S26.** DSC thermogram of formulation **F12**. In this formulation, *i*BuMACC was employed instead of DMACC.

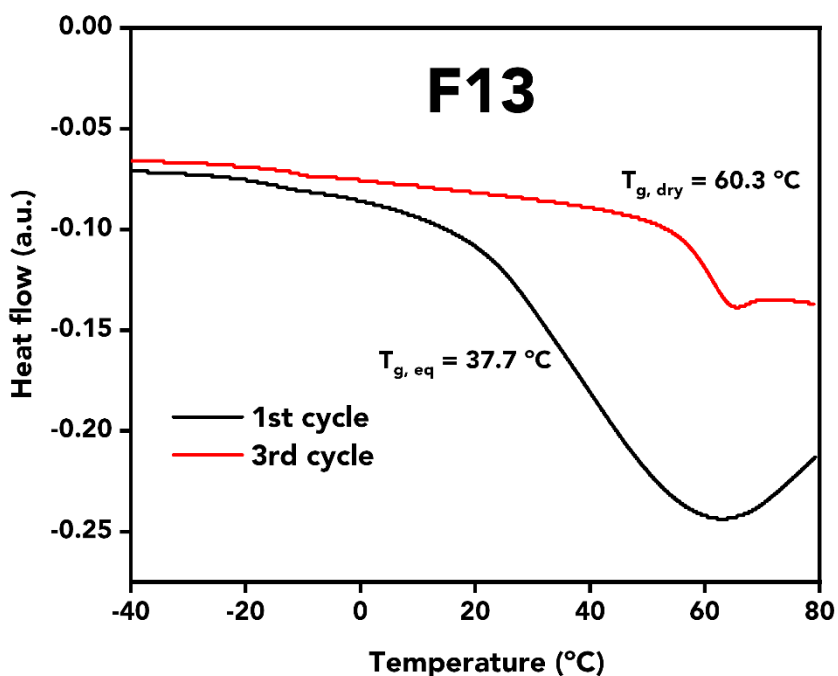


**Figure S27.** DSC thermogram of formulation **F13**. In this formulation, CHACC was employed instead of DMACC.

## Supporting Information

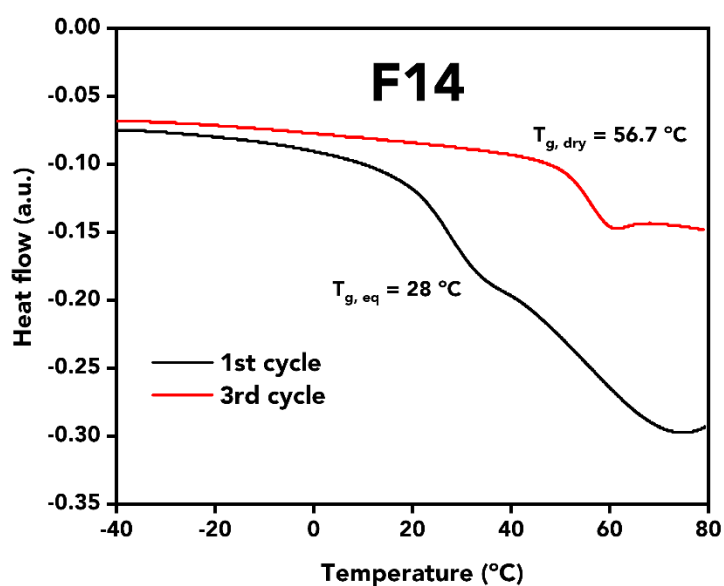


**Figure S28.** DSC thermogram of formulation **F14**. In this formulation, MPACC was employed instead of DMACC.

### 3.5.1.3. TGA analysis

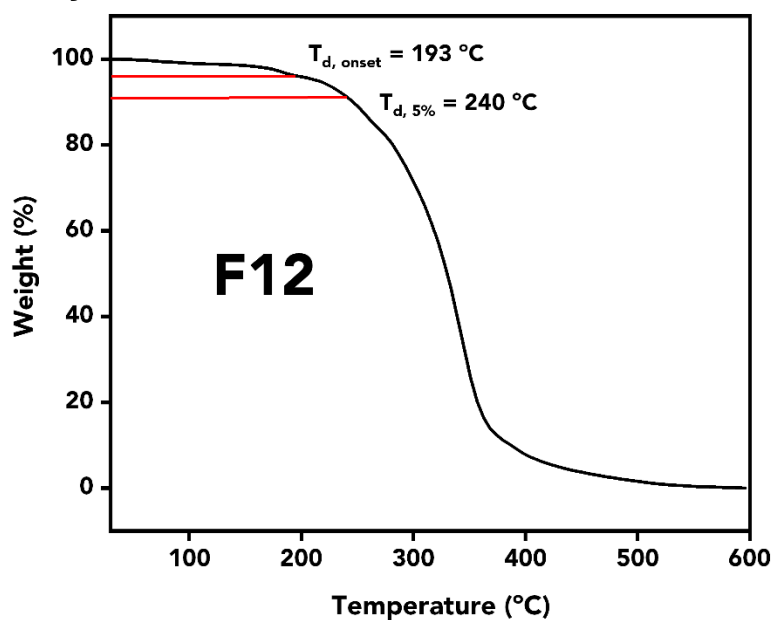


**Figure S29.** TGA thermogram of formulation **F12**. In this formulation, iBuMACC was employed instead of DMACC.

## Supporting Information

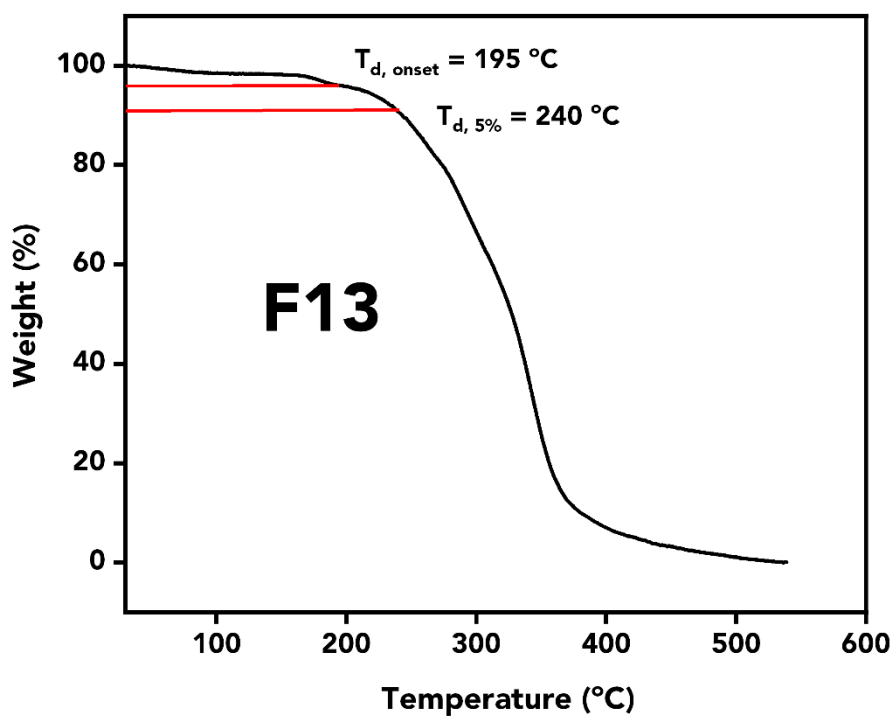


**Figure S30.** TGA thermogram of formulation **F13**. In this formulation, CHACC was employed instead of DMACC.

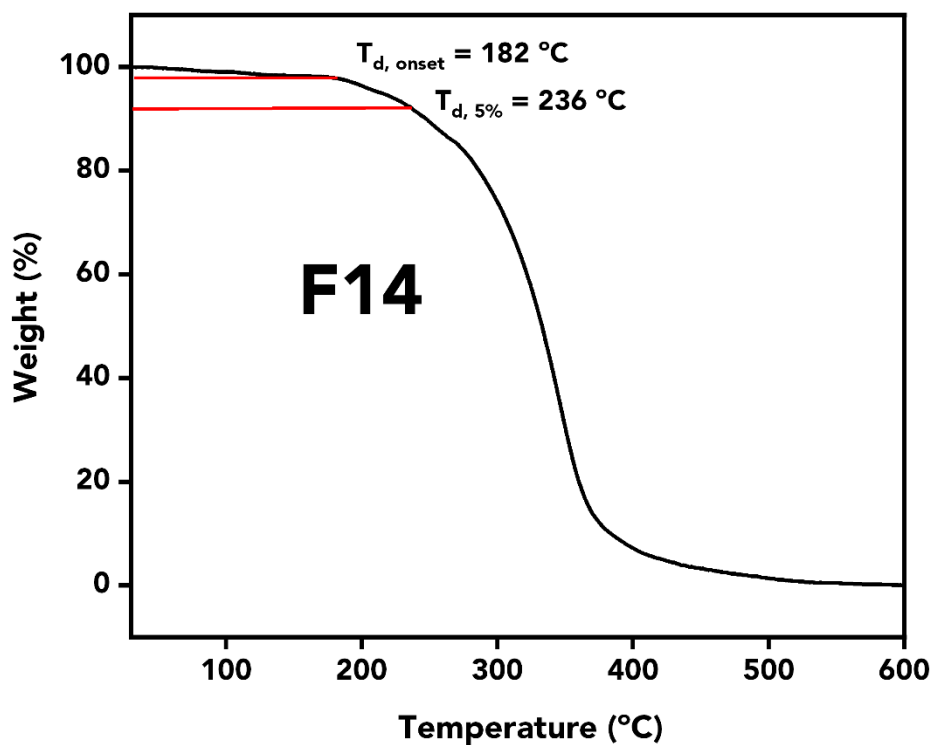


**Figure S31.** TGA thermogram of formulation **F14**. In this formulation, MPACC was employed instead of DMACC.



## Supporting Information

### 3.5.2. Formulations with different amines mixture.

#### 3.5.2.1. FT-IR analysis

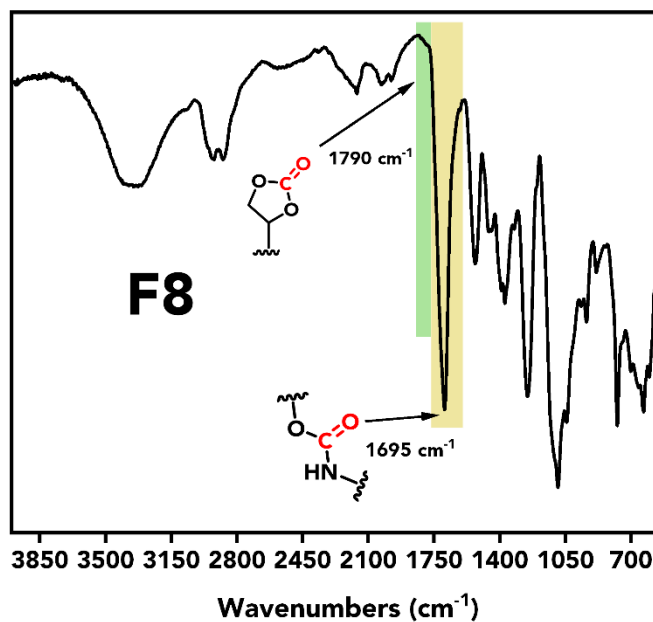


**Figure S32.** FT-IR spectra of formulation **F8**. In this formulation, an amine mixture was introduced with 70 mol% of TREN and 30 mol% of mXDA.

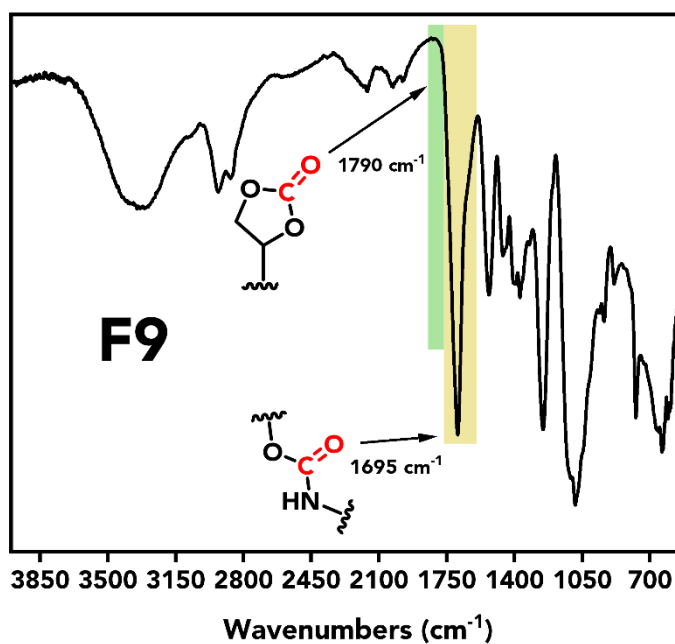


**Figure S33.** FT-IR spectra of formulation **F9**. In this formulation, an amine mixture was introduced with 70 mol% of TREN and 30 mol% of HMDA.

## Supporting Information

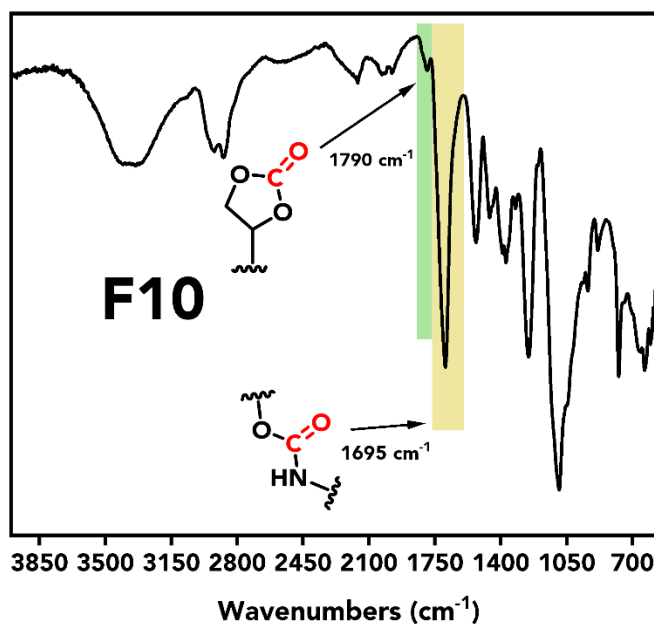


**Figure S34.** FT-IR spectra of formulation **F10**. In this formulation, an amine mixture was introduced with 70 mol% of TREN and 30 mol% of EDR-148.

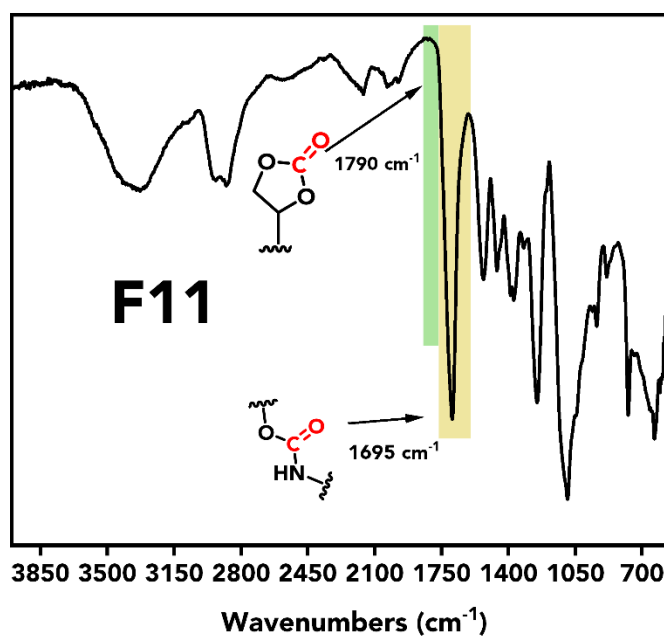


**Figure S35.** FT-IR spectra of formulation **F11**. In this formulation, an amine mixture was introduced with 70 mol% of TREN and 30 mol% of IPDA.

## Supporting Information

### 3.5.2.2. DSC analysis

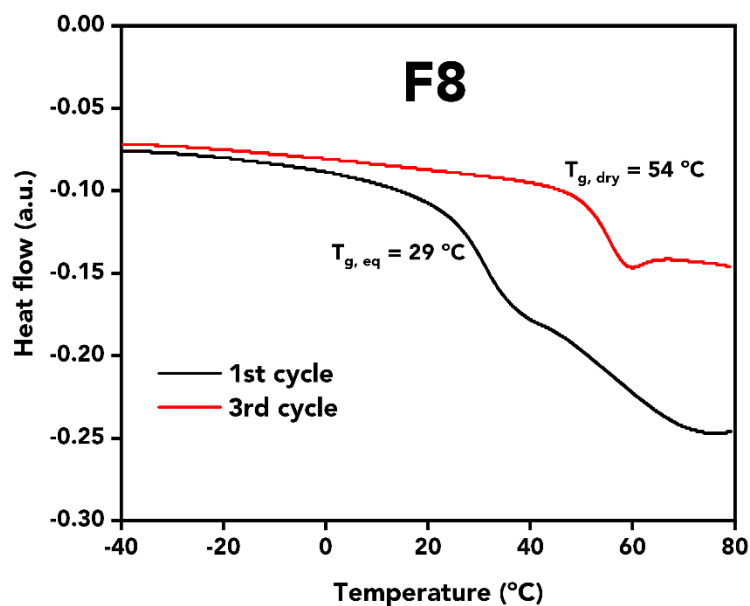


**Figure S36.** DSC thermogram of formulation **F8**. In this formulation, an amine mixture was introduced with 70 mol% of TREN and 30 mol% of mXDA.

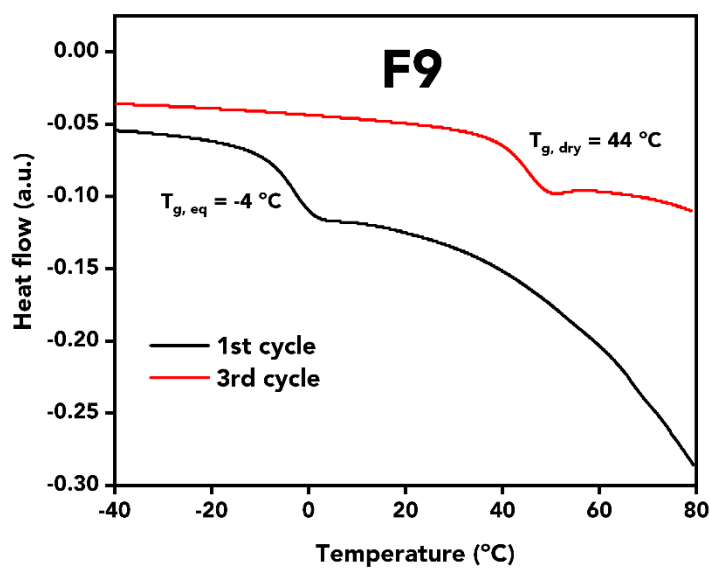


**Figure S37.** DSC thermogram of formulation **F9**. In this formulation, an amine mixture was introduced with 70 mol% of TREN and 30 mol% of HMDA.

## Supporting Information

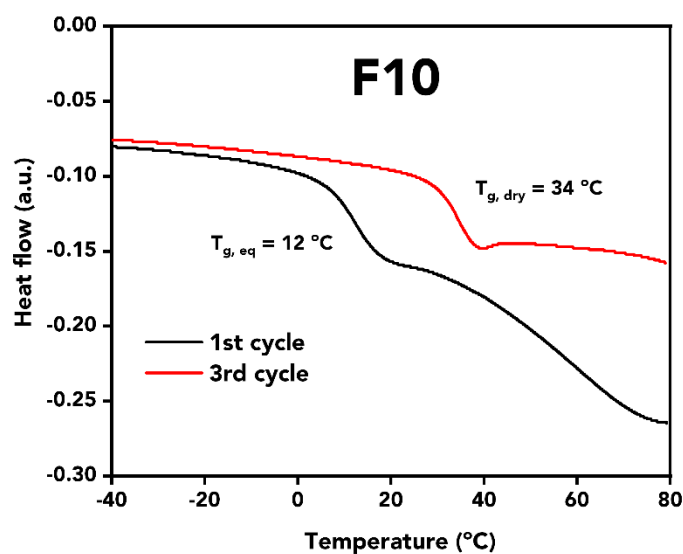


**Figure S38.** DSC thermogram of formulation **F10**. In this formulation, an amine mixture was introduced with 70 mol% of TREN and 30 mol% of EDR-148.

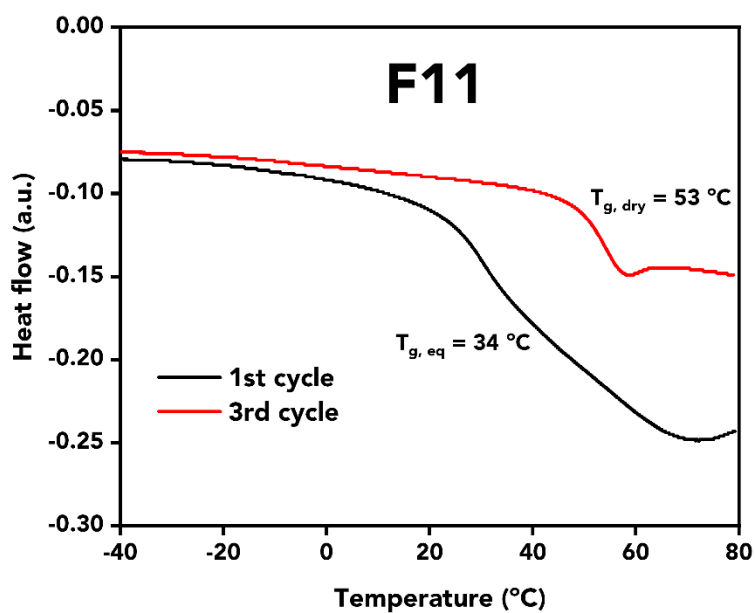


**Figure S39.** DSC thermogram of formulation **F11**. In this formulation, an amine mixture was introduced with 70 mol% of TREN and 30 mol% of IPDA.

## Supporting Information

### 3.5.2.3. TGA analysis

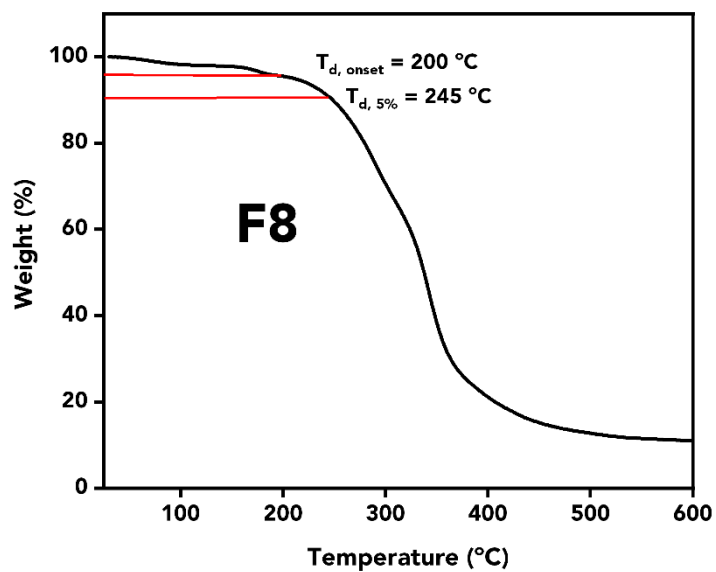


**Figure S40.** TGA thermogram of formulation **F8**. In this formulation, an amine mixture was introduced with 70 mol% of TREN and 30 mol% of mXDA.

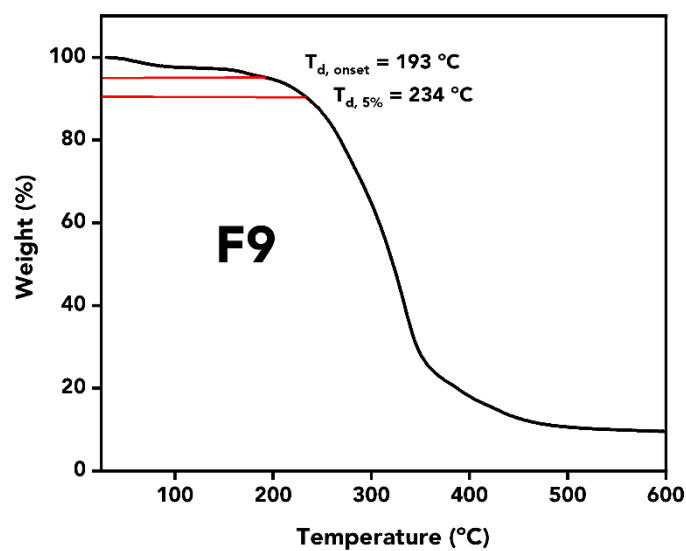


**Figure S41.** TGA thermogram of formulation **F9**. In this formulation, an amine mixture was introduced with 70 mol% of TREN and 30 mol% of HMDA.

## Supporting Information

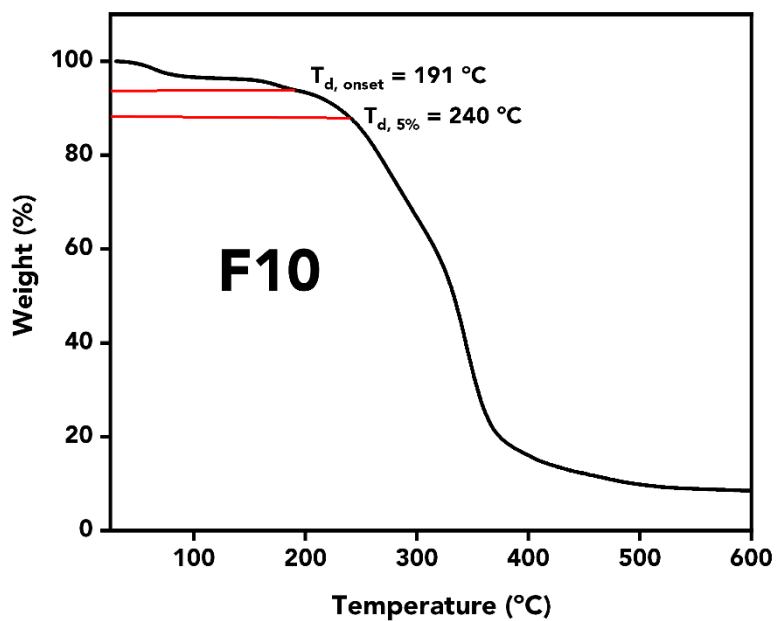


**Figure S42.** TGA thermogram of formulation **F10**. In this formulation, an amine mixture was introduced with 70 mol% of TREN and 30 mol% of EDR-148.

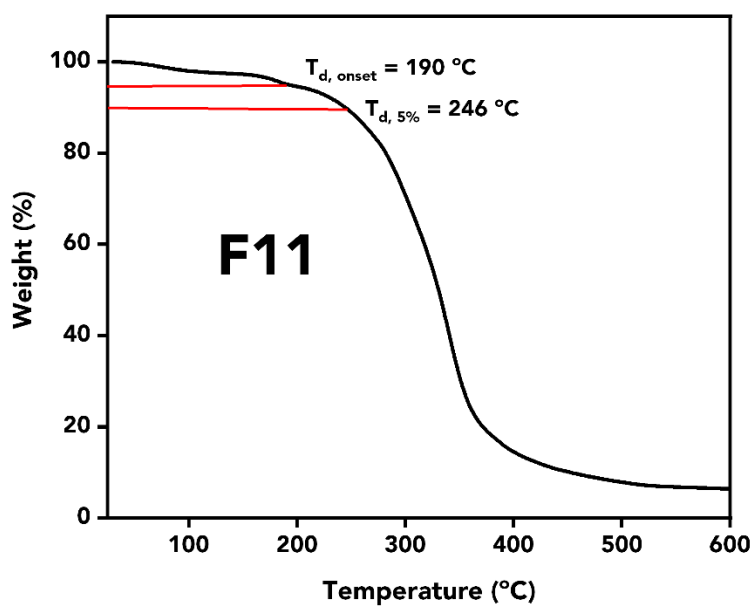


**Figure S43.** TGA thermogram of formulation **F11**. In this formulation, an amine mixture was introduced with 70 mol% of TREN and 30 mol% of IPDA.

## Supporting Information

### 3.5.2.4 Exotherm recorded depending on amine ratio of TREN to diamine used in the formulation

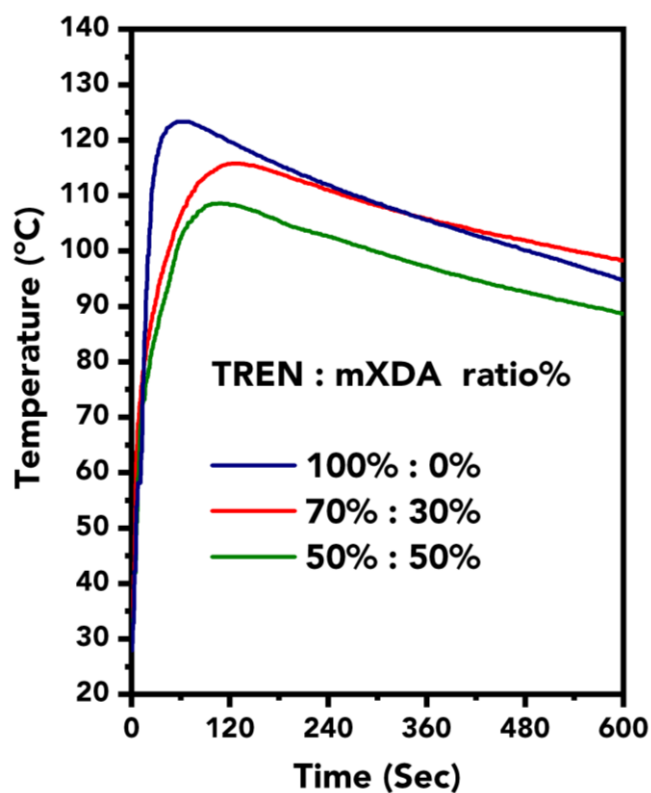


**Figure S44.** Temperature vs. time plot in with different amine ratios.

### 3.6. Compression tests

**Table S6.** Calculated Young's Modulus from Compression Tests Performed on NIPUFs with Different Formulations, Equilibrated at Set Humidity Levels; (See Table 1, and S2-3 in ESI for all formulations; section 6.3.3. for NIPUF synthesis conditions).

Foam	Density, (kg × m <sup>-3</sup> )	Young's Modulus (MPa) vs. Humidity (%)				T <sub>g,dry</sub> °C
		Dry	40	60	80	
F6	118 ± 4	8.54	1.66	0.040	0.020	46.5
F9	112 ± 5	0.30	0.02	0.003	0.002	44
F8	121 ± 3	9.00	8.90	0.030	0.004	54

## Supporting Information

### 4. $\alpha$ CC monomer synthesis

#### 4.1. DMACC monomer synthesis

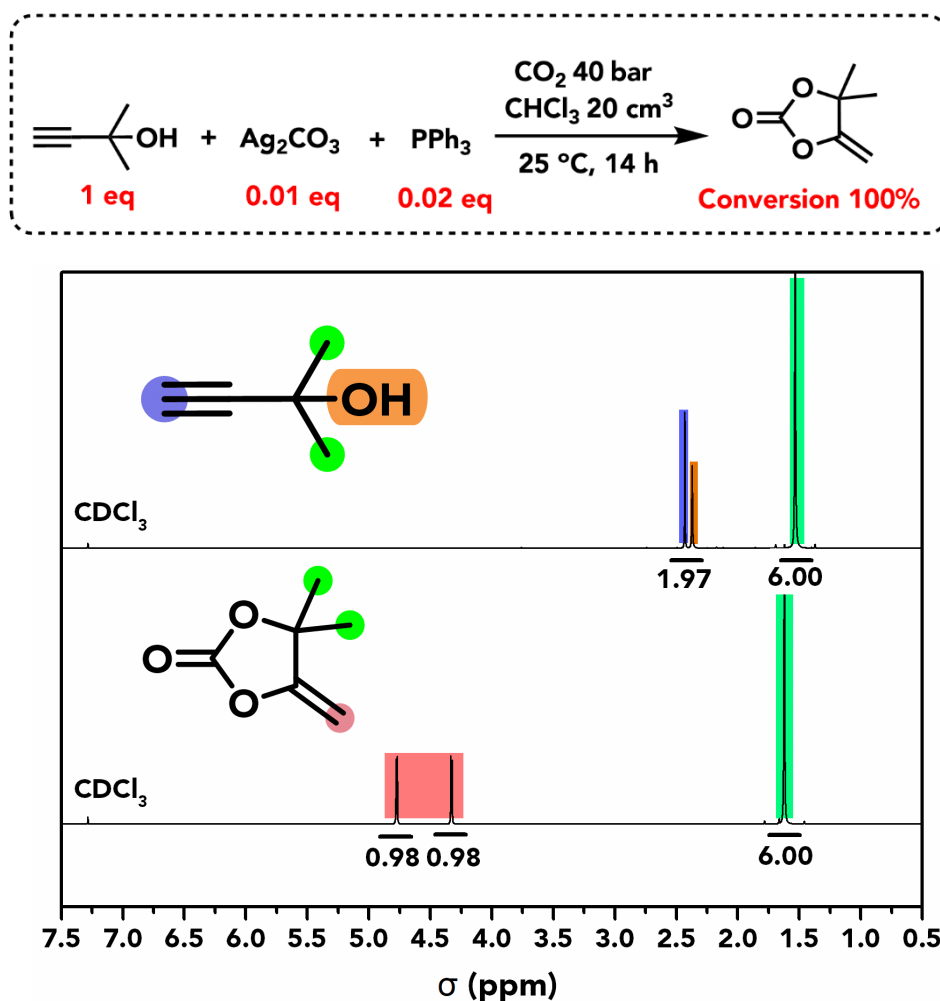


**Figure S45.** Assigned, stacked  $^1\text{H}$ -NMR spectra of DMACC monomer and its precursor.

In a 250 mL high-pressure autoclave, 2-methyl-3-butyn-2-ol (125  $\text{cm}^3$ , 1.3 mol, 1 eq.),  $\text{Ag}_2\text{CO}_3$  (3.585 g, 0.013 mmol, 0.01 eq.), triphenylphosphine (6.82 g, 0.026 mmol, 0.02 eq.), and 20 mL of chloroform were combined. The reactor was then charged with 40 bars of  $\text{CO}_2$  at room temperature ( $25^\circ\text{C}$ ). After 14 h, the reaction mixture was depressurized and subjected to vacuum distillation. The resulting transparent liquid was dissolved in diethyl ether and washed with water to remove impurities. The organic layer was dried over magnesium sulfate, filtered, and concentrated under vacuum. The product crystallized as a white solid upon further drying (yield: 91%). The melting point was determined to be  $26^\circ\text{C}$ .  $^1\text{H}$ -NMR (400 MHz,  $\text{CDCl}_3$ ) and FT-IR analyses confirmed the conversion of the product.



## Supporting Information

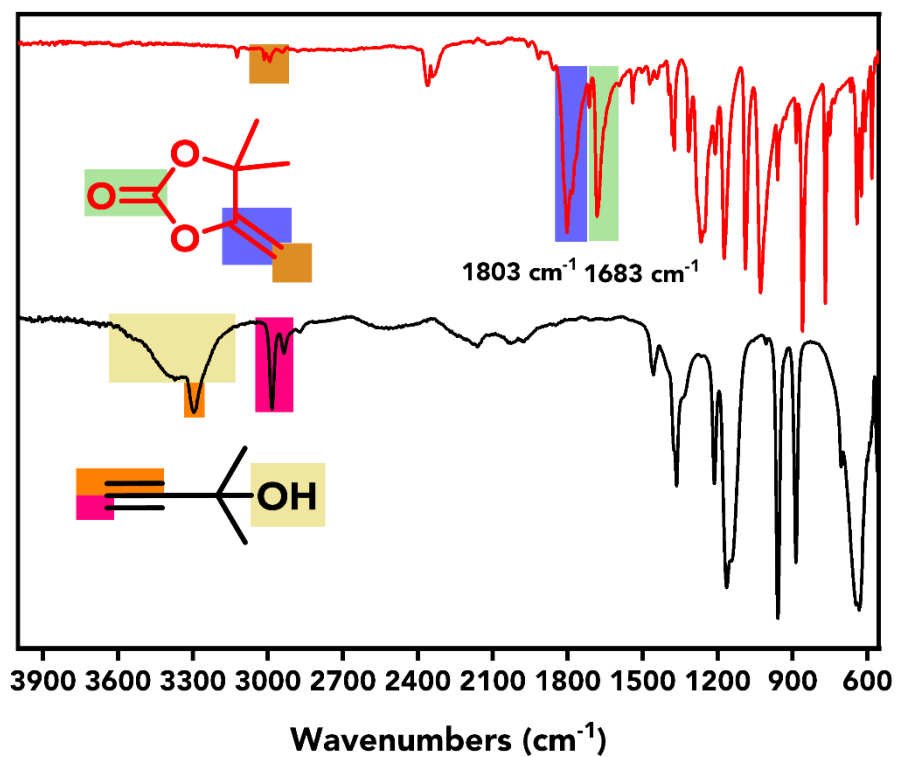


*Figure S46. Stacked FT-IR spectra of DMACC and its precursor.*

## Supporting Information

### 4.2. CHACC monomer synthesis

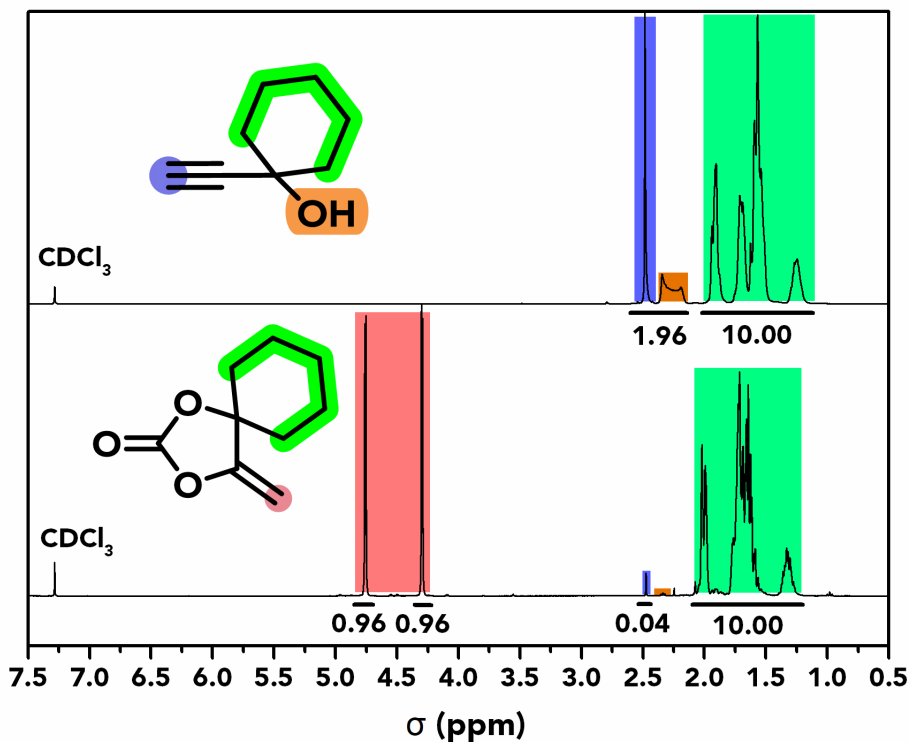
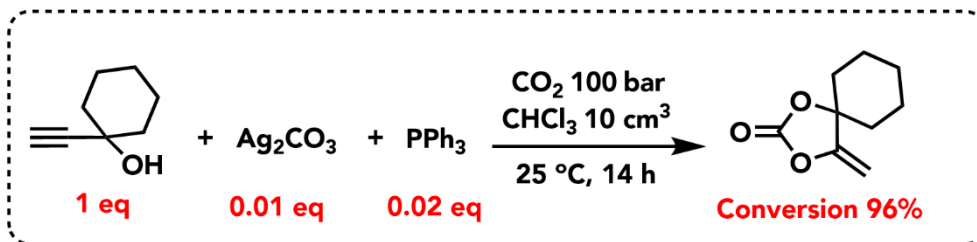


**Figure S47.** Assigned, stacked  $^1\text{H}$ -NMR spectra of CHACC monomer and its precursor.

In a 250 mL high-pressure autoclave, 1-ethynylcyclohexan-1-ol (40 cm<sup>3</sup>, 0.31 mol, 1 eq.),  $\text{Ag}_2\text{CO}_3$  (1.65 g, 0.006 mmol, 0.02 eq.), triphenylphosphine (3.15 g, 0.012 mmol, 0.04 eq.), and 10 mL of chloroform were combined. The reactor was then charged with 100 bars of  $\text{CO}_2$  at room temperature (25°C). After 14 h, the reaction mixture was depressurized and subjected to vacuum distillation. The following purification step was the same as in the case of DMACC. The product was a transparent, colorless liquid (yield: 90%).  $^1\text{H}$ -NMR (400 MHz,  $\text{CDCl}_3$ ) and FT-IR analyses confirmed the conversion of the product.

## Supporting Information

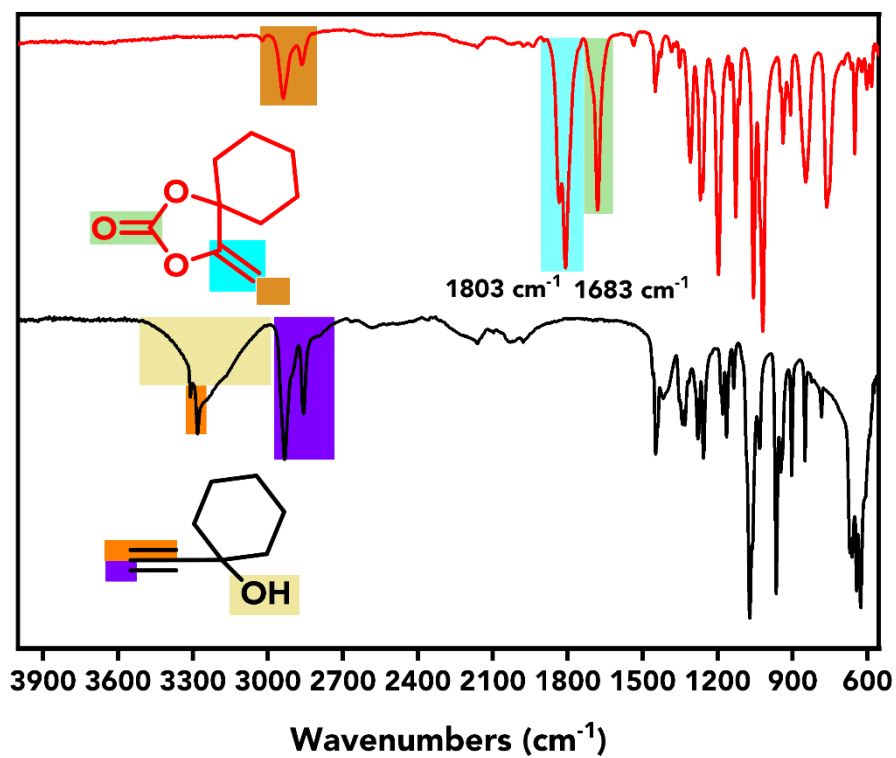


**Figure S48.** Stacked FT-IR spectra of CHACC and its precursor.

## Supporting Information

### 4.3. iBuMACC monomer synthesis

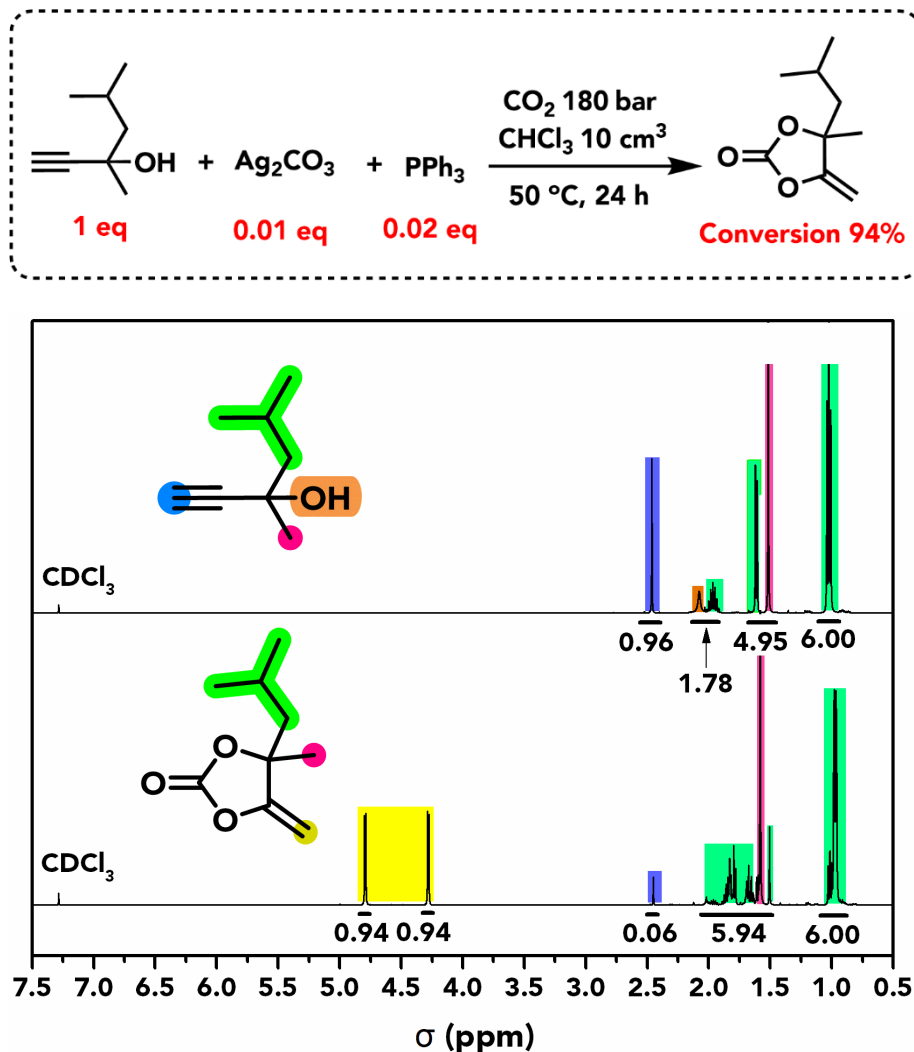


**Figure S49.** Assigned, stacked  $^1\text{H}$ -NMR spectra of iBuMACC monomer and its precursor.

In a 250 mL high-pressure autoclave, 3,5-Dimethyl-1-hexyn-3-ol (40  $\text{cm}^3$ , 0.27 mol, 1 eq.),  $\text{Ag}_2\text{CO}_3$  (1.65 g, 0.006 mmol, 0.02 eq.), triphenylphosphine (3.15 g, 0.012 mmol, 0.04 eq.), and 10 mL of chloroform were combined. The reactor was then charged with 180 bars of  $\text{CO}_2$  at room temperature (25 $^\circ\text{C}$ ). After 24 h, the reaction mixture was depressurized and subjected to vacuum distillation. The following purification step was the same as in the case of DMACC. The product was a transparent, colorless liquid (yield: 88%).  $^1\text{H}$ -NMR (400 MHz,  $\text{CDCl}_3$ ) and FT-IR analyses confirmed the conversion of the product.

## Supporting Information

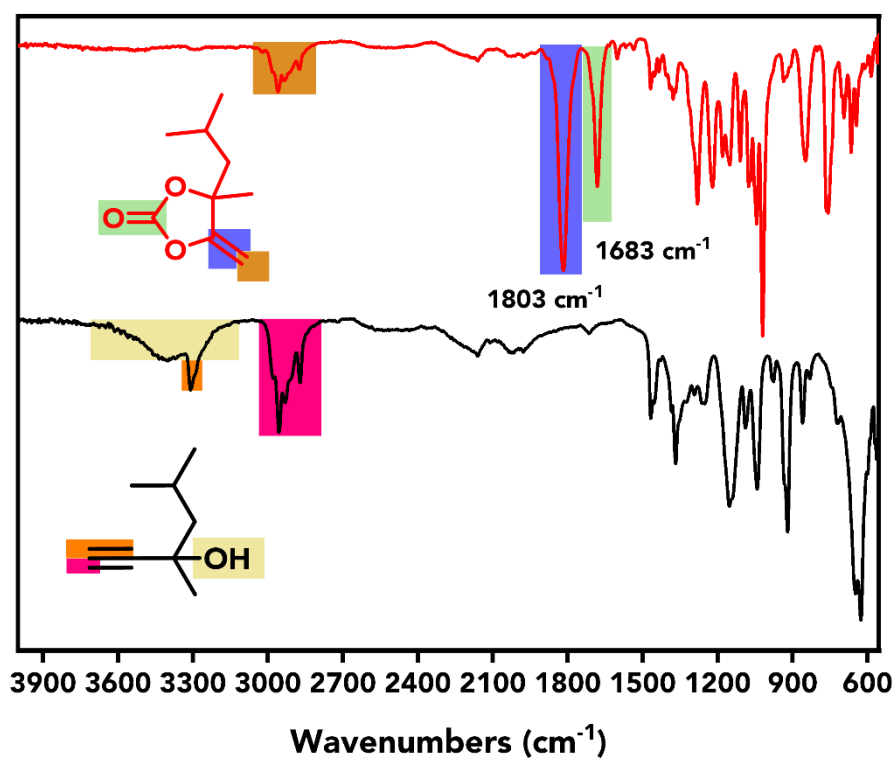


**Figure S50.** Stacked FT-IR spectra of iBuMACC and its precursor.

## Supporting Information

### 4.4. MPACC monomer synthesis

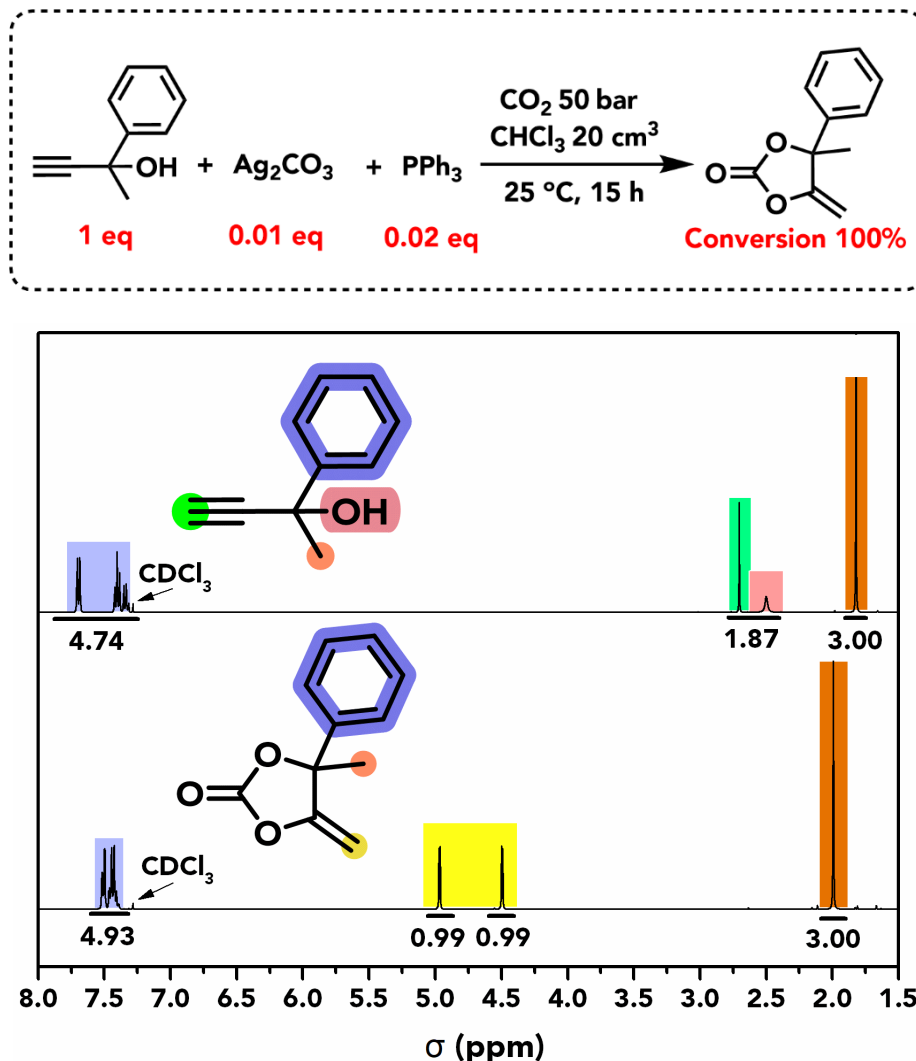


**Figure S51.** Assigned, stacked  $^1\text{H}$ -NMR spectra of MPACC monomer and its precursor.

In a 250 mL high-pressure autoclave, 2-phenyl-3-butyn-2-ol (25 g, 0.17 mol, 1 eq.),  $\text{Ag}_2\text{CO}_3$  (0.47 g, 0.002 mol, 0.01 eq.), triphenylphosphine (0.892 g, 0.003 mol, 0.02 eq.), and 20 mL of chloroform were combined. The reactor was then charged with 50 bars of  $\text{CO}_2$  at room temperature (25  $^\circ\text{C}$ ). After 15 h, the reaction mixture was depressurized and subjected to vacuum distillation. The following purification step was the same as in the case of DMACC. The product crystallized as a white solid upon further drying (yield: 90%). The melting point (mp) was determined to be 27  $^\circ\text{C}$ .  $^1\text{H}$ -NMR (400 MHz,  $\text{CDCl}_3$ ) and FT-IR analyses confirmed the conversion of the product.

## Supporting Information

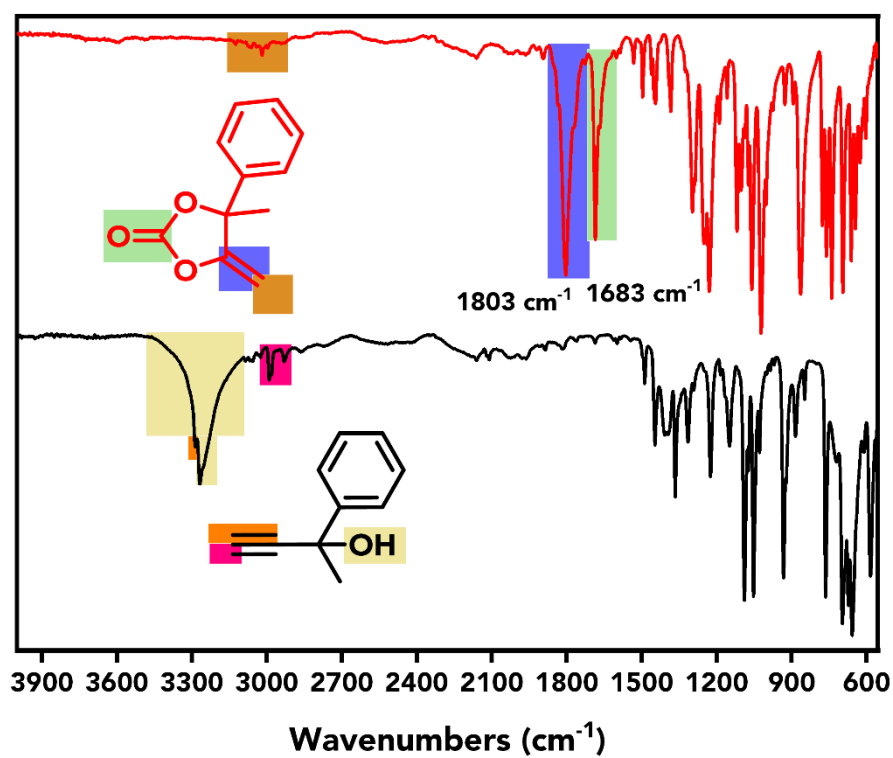


**Figure S52.** Stacked FT-IR spectra of MPACC and its precursor.